Supplementary Information

A Rationally Designed Peptoid for the Selective Chelation of Zn^{2+} Over Cu^{2+}

Pritam Ghosh and Galia Maayan*
Schulich Faculty of Chemistry, Technion-Israel Institute of Technology, Technion City, Haifa 3200008, Israel, E-mail: gm92@technion.ac.il

Materials

Rink Amide resin was purchased from Novabiochem. 2-([2,2':6',2"-terpyridin]-4'-yloxy)ethan-1-amine (Netp) has been synthesized as per the literature report[1] where precursor 4'-bromo-2,2':6',2"-terpyridine was purchased from Alfa Aesar and ethanolamine from Acros organics, Israel. Reagents like piperdine, 2-picolyl amine, (Aminomethyl)cyclohexane, Amyl amine and allyl amine were purchased from Sigma Aldrich. Benzylamine, 1-(Aminomethyl)naphthalene were purchased from ACROS Organics. (R)-(-)-3,3-Dimethyl-2-butylamine was procured from Alfa Aesar Chemical company. Aryl amine was purchased from Merck. N,N'-diisopropylcarbodiimide (DIC) was purchased from Chem-Impex Int'l Inc. Bromoacetic acid was purchased from Merck and chloro acetic acid was from Acros organics. Metal salts are purchased of analytical grade. All used solvents were HLPC grade of which dimethylforamide (DMF), toluene and dichloromethane (DCM) solvents were purchased from Bio-Lab Ltd. Acetonitrile (ACN) and water were obtained from Sigma-Aldrich.

Instrumentations

Reversed-phase HPLC on a Jasco UV-2075 instrument (analytical C18 column, Luna 5µm, 100 Å, 2.0 x 50 mm) was used to analyze synthesized peptoids. Linear gradient of 5–95% ACN in water with 0.1% TFA (flow rate is 700 µL/min) over 10 min was used. Preparative HPLC was performed using a phenomenex C18 column (Luna 15µm, 100 Å 21.20x100mm) on a Jasco UV-2075 instrument using 5–95% ACN in water with 0.1% TFA as solvent for elution. A linear gradient of the solvent is used over 50 min at a flow rate of 5 mL/min. Mass spectrometry was performed on Waters LCT Premier mass [ESI+, direct probe ACN:H_2O (95:5), flow rate 0.2 ml/min] and Advion expression mass under electrospray ionization (ESI) [ESI+, direct probe ACN:H_2O (70:30), flow rate 0.3 ml/min]. ^{1}H-NMR spectra were recorded using an AVANCE II 400 MHz Bruker spectrometer. Proton chemical shifts are expressed in parts per million (ppm, δ scale) and are referenced to teramethylsilane ($(CH_3)_4Si$, 0.00 ppm). Circular Dichroism experimentation was carried out using Applied Photophysics chirascan spectrophotometer. EPR spectra were using a Bruker EMX-10/12 X-band (ν=9.4 GHz) digital EPR spectrometer. Spectra processing and simulation were carried out with the Bruker WIN-EPR and SimFonia Software. The g factors values were determined using 2,2,6,6- tetramethylpiperidine-N-oxyl (TEMPO) as reference (g = 2.0058). Kaleida Graph is used for data processing.

Preparation of peptoid oligomers

Peptoids (**PT-1-9** and **PD-1**) were manually prepared in fritted syringes by the sub-monomer method on Rink amide resin at room temperature.[2] In a typical synthesis, rink-amide resin (100 mg) was measured

and swallowed in DCM for a period of 40 minutes. De-protection of the resin was carried out by piperidine solution (20%, solvent: DMF) followed by 20 minutes shaking in ambient condition. Next, piperidine was washed by DMF for three times with one minute duration (1 mL/ 25 mg resin each time). Bromoacetylation was done by addition of 20 eq. Bromoacetic acid (1.2 M in DMF, 8.5 mL/g resin) together with 24 eq. of diisopropylcarbodiimide (2 mL g^{-1} resin), shaking for 20 min in room temperature. Afterwards, the bromoacetylation reagents were properly washed from the resin by DMF (1 mL/ 25 mg resin each time, three times with one minute duration each time). After washing, 20 eq. of the primary amine (1.0 M in DMF, 10 mL/g resin) was added under shaking for next 20 minutes at room temperature and later washed three times by DMF. Bromoacetylations and amine displacement steps were repeated till the desired sequence was loaded on the resin. In case of picolyl amine step, chloroacetic acid was used instead of bromoacetic acid.[3] When the synthesis of the desired sequence was finished, they were cleaved from solid support for initial analysis. Approximately 4-6 mg of the resin were dispersed in a cleavage cocktail solution (TFA:DCM:Water= 4.9:4.9:0.2) for 30 minutes.[3] Then the cleavage solution was evaporated under nitrogen flow and the residue is suspended in 0.5 mL HPLC grade 1:1 water and acetonitrile mixture. To cleave the entire peptoid oligomers from the solid support for preparative HPLC, the beads were dispersed in the cleavage cocktail solution (TFA:DCM:Water= 4.9:4.9:0.2) for 90 minutes. The solution was evaporated under low pressure, solubilized in 5 mL HPLC grade 1:1 water and acetonitrile mixture and lyophilized overnight.

Characterization of the peptoid oligomers

The peptoids (**PT-1-9** and **PD-1**) were characterized by analytical HPLC using a C18 column using a specific solvent gradient of 5% to 95% solvent B (0.1% TFA in HPLC grade acetonitrile) over solvent A (0.1% TFA in HPLC grade water) for 10 minutes under a constant flow rate of 0.7 mL/min with 214 nm UV absorbance. In case of preparative HPLC at 230 nm, C18 column was used where the solvent gradient was 5% to 95% solvent B (0.1% TFA in HPLC grade acetonitrile) over solvent A (0.1% TFA in HPLC grade water), duration 50 minutes, flow rate 5 mL/min. The collected peptoids were lyophilized overnight. The pure peptoids were further analysed by RP-HPLC [C18 column with a linear gradient of 5–95% ACN in water (0.1% TFA) over 10 min at a flow rate of 700 µL/min and 214 nm UV absorbance].
PT-1 Proton (^{1}H) NMR (δ in ppm) (400 MHz; ACN-d_3): 9.30(s, 1H, -NH, *N*-terminal end), 9.18 (m, 3H, Ar-H), 8.84 (d, 1H, Ar-H), 8.77 (d, 1H, Ar-H), 8.63 (m, 3H, Ar-H), 8.27 (d, 1H, Ar-H), 8.06 (m, 2H, Ar-H), 7.92 (m, 1H, Ar-H), 6.30 (m, 2H, -NH_2, *C*-terminal end), 7.4 (m, 8H, Ar-H), 4.55 (m, 9H, -CH_2 of skeletal and linker), 3.97 (m, 5H, -CH_2 of skeletal and linker) (Fig. S53a).

Table S1. Peptoid oligomer sequences with their molecular weights and UV-Vis signals. [*N*pm: phenylmethanamine; *N*nap: naphthalen-1-ylmethanamine; *N*chm: cyclohexylmethanamine; *N*rtb: (R)-3,3-dimethylbutan-2-amine ; *N*pen: pentan-1-amine; *N*all: prop-2-en-1-amine; *N*me: 2-methoxyethan-1-amine; *N*etp: 2-([2,2':6',2"-terpyridin]-4'-yloxy)ethan-1-amine; *N*pam: pyridin-2-ylmethanamine; Ac: acetylated]

Entry	Peptoid oligomers	Molecular weight	λ_{max} (UV-Vis analysis)
		Calc: Found	8 μM solvent: water
1	**PT-1** (*N*pm- *N*etp- *N*pam)	644.29: 645.35	235, 262 and 275 nm
2	**PT-1Ac** (*N*pm- *N*etp- *N*pam-Ac)	686.30: 687.28	234, 261, 267 and 277 nm
3	**PT-2** (*N*nap- *N*etp- *N*pam)	694.30: 695.71	222, 266 and 280 nm
4	**PT-3** (*N*chm- *N*etp- *N*pam)	650.33: 651.61	233, 266 and 277 nm
5	**PT-4** (*N*rtb- *N*etp- *N*pam)	638.33: 639.44	234, 268 and 276 nm
6	**PT-5** (*N*pen- *N*etp- *N*pam)	624.32: 625.47	234, 258, 266 and 277 nm
7	**PT-6** (*N*all- *N*etp- *N*pam)	594.27: 595.22	234, 266 and 275 nm
8	**PT-7** (*N*me- *N*etp- *N*pam)	612.28: 613.67	235 and 276 nm
9	**PT-8** (*N*pm- *N*etp- *N*pm)	643.29: 644.27	235 and 276 nm
10	**PD-1** (*N*etp- *N*pam)	497.22: 498.16	235, 259, 267 and 277 nm

Synthesis of Copper/ Zinc peptoid complexes

Lyophilized **PT-1** (0.05 mmol) was dissolved in water (2 mL) and stirred for 10 minutes. The solution was colorless. Copper acetate monohydrate or zinc acetate dihydrate (0.05 mmol as solid) was added to the solution of the peptoid under stirring condition and kept for next 4 hours in room temperature. During the reaction with copper, the reaction mixture turns blue while during the reaction with zinc no color change has been observed. The solution was lyophilized to obtain the complex.

Synthesis of Zn**PT-1** and Cu**PT-1** in different temperatures: To a vile containing 500 μL water solution of **PT-1** (1mM), one equivalent metal ion (Zn^{2+} or Cu^{2+}, stock solution in water, 50 mM) was added in either room temperature, 35°C or 50°C and stirred for 24 hours. The reaction was monitored by UV-Vis.

Synthesis of Zn**PT-1** and Cu**PT-1** in different solvents: The reaction was carried out in room temperature for four hours in acetonitrile and/or methanol. Concentration was maintained at 17 μM. The UV-Vis response was remained almost similar other than 2 nm shift in 245 nm peak of Zn**PT-1** (H_2O) that was shifted to 247 nm in Zn**PT-1** (ACN).

Characterization of Zn**PT-1**: Yield: 92%, ESI-MS: calculated for [Zn^{2+}-**PT-1**+OAc^-] 767.23, found: 767.2338, assigned with proper isotope labelling. UV-Vis characterization (17 μM in water), λ_{max} for

Zn**PT-1** are 245, 267, 275, 310 and 322 nm. FT-IR peaks (υ, cm^{-1}): 3085, 2948, 1666, 1537, 1440, 1192, 1136, 954, 719, 693. [UV-Vis: Fig. S41, ESI-MS: Fig. S43, FT-IR: Fig. S54c]. λ_{max} for Zn**PT-1** in acetonitrile are 247, 267, 276, 310 and 323 nm; λ_{max} for Zn**PT-1** in methanol are 246, 268, 275, 312 and 323 nm (Fig. S47).

Characterization of Cu**PT-1**: Yield: 88%, ESI-MS: calculated for [Cu^{2+}-**PT-1**+OAc^-+K^+] 805.19, found: 805.10, assigned with proper isotope labelling. UV-Vis characterization (17 μM in water), λ_{max} for Cu**PT-1** are 253, 259, 279, 318, 329 and 665 (d-d) nm. FT-IR peaks (υ, cm^{-1}): 3093, 2952, 1654, 1597, 1421, 1190, 1140, 1030, 792, 685. Hamiltonian parameter in EPR, for frozen solution g_{II}: 2.22; $g_{\perp}$: 2.06; A_{II}: 165G. [UV-Vis: Fig. S42, ESI-MS: Fig. S44, FT-IR: Fig. S54b, EPR: Fig. S55]. λ_{max} for Cu**PT-1** in acetonitrile are 253, 260, 279, 318 and 330 nm; λ_{max} for Cu**PT-1** in methanol are 253, 259, 279, 318 and 330 nm (Fig. S47).

The UV-Vis peaks of Zn^{2+}/Cu^{2+}-peptoids are summarised below:

Table S2. UV-Vis absorbance data of peptoid oligomers and it Zn^{2+}/Cu^{2+} complexes in water.

Sl No	Peptoid oligomers	λ_{max} (UV-Vis analysis for Zn^{2+} complex)	λ_{max} (UV-Vis analysis for Cu^{2+} complex)
		8 μM solvent: water	8 μM solvent: water
1	**PT-1**	245, 267, 275, 310 and 322 nm	253, 259, 279, 318, 329 and 665 (d-d) nm
2	**PT-1Ac**	243, 267, 272, 309 and 321 nm	241, 255, 266, 275, 315 and 327 nm
3	**PT-2**	222, 243, 270, 310 and 322 nm	220, 258, 277, 316 and 328 nm
4	**PT-3**	243, 274, 282, 309 and 322 nm	258, 275, 316 and 328 nm
5	**PT-4**	243, 273, 284, 309 and 322 nm	248, 274, 315 and 327 nm
6	**PT-5**	243, 266, 273, 309 and 322 nm	257, 276, 303, 315 and 327 nm
7	**PT-6**	243, 268, 275, 309 and 321 nm	258, 276, 316 and 328 nm
8	**PT-7**	243, 266, 274, 296, 309 and 321 nm	252, 276, 302, 316 and 328 nm
9	**PT-8**	243, 275, 313 and 322 nm	250, 275, 315 and 328 nm
10	**PD-1**	243, 260, 266, 272, 309 and 322 nm	240, 268, 275, 315 and 328 nm

UV-Vis titration experiment for peptoids

After recording the blank spectrum of water in 200-800 nm range, 10 μL of peptoids (5 mM stock solution) was added into 3mL of water, taken in a standard cuvette used for UV-Vis absorbance analysis to obtain a concentration of 16.61 μM, ~17 μM. Later Zn^{2+} and Cu^{2+} was titrated separately to obtain the absorbance of individual complexes for **PT-1** by addition of 2 μL metal solution, 2 mM in water stock solution. It shows distinct change in 300-350 nm peak after one equivalent of metal ion addition,

suggesting 1:1 complexation (peptoid:metal). For further insight, ESI-MS of the metal ion titrated solution as obtained from UV-Vis titration was carried out which also shows 1:1 complexation (Fig. S25 and S26b).

UV-Vis competition experiments

The competition experiments of peptoids with metal ions (Cu^{2+}, Zn^{2+}) were carried out in water medium. The stock solution of peptoid and metal ions were prepared at 5 mM concentration. The UV-Vis of Zn^{2+}-peptoid and Cu^{2+}-peptoid complex shows signal at different wavelength for these two complexes. Now, a mixture for competition experiment was prepared. In an Eppendorf, 5μL of Zn^{2+} and 10μL Cu^{2+} (1:2 ratio) was taken and mixed. Later this mixture was added at-a-time to the cuvette containing the peptoid. Now the UV-Vis of the peptoid with the mixture of metal was recorded. The peak between 300-350 nm was mainly monitored which could show the nature of the complex formed in solution. Finally this solution was monitored by ESI-MS to confirm the complexation.

Dissociation constants calculations

The dissociation constants for Zn^{2+} with the peptoids **PT-1**, **PT-2** and **PT-3**) were measured by using UV-Vis spectroscopy following a competition method. The stock solution of the peptoids, EDTA and Zn^{2+} were prepared at 5 mM concentration in water. For EDTA, the pH was maintained at 7 by adding NaOH (5 mM in water). In a typical competition experiment,[4] each peptoid (individually) and EDTA were mixed in a 1:1 ratio at 26.53 μM (15 μL 5 nM from each solution in 3 mL of water) in a UV-Vis cuvette and gradually titrated with Zn^{2+} up to one equivalent as examined peptoids bind one equivalent of metal ion. The UV-Vis spectra was monitored at 300-350 nm range. Following the method reported by Wedd and Xiao *et al*, the slope between $\{([Peptoid]_{tot}/[Zn^{2+}\text{-Peptoid}])-1\}$ and $\{([EDTA]_{tot}/[Zn^{2+}\text{-EDTA}])-1\}$ was calculated. The value of the slope is equal to $K_{d(Zn^{2+}\text{-Peptoid})}K_{a(Zn^{2+}\text{-EDTA})}\alpha_{(EDTA)}$ where $K_{d(Zn^{2+}\text{-Peptoid})}$ is the dissociation constant of Zn^{2+}-peptoid, $K_{a(Zn^{2+}\text{-EDTA})}$ is the association constant of Zn^{2+}-EDTA complexation and $\alpha_{(EDTA)}$ is the pH correction factor for EDTA.

Table S3 is showing an example of how the slope was calculated for Zn^{2+} competition with **PT-1** and EDTA. Total concentration of **PT-1** and EDTA were kept as 26.53 μM. The absorbance of EDTA free **PT-1** (26.53 μM) titrated with Zn^{2+} was used to calculate the unknown concentration of Zn**PT-1** formed in presence of EDTA *via* Beer–Lambert law. The unknown concentration is referred here to Zn-Peptoid in Table S3, 5th column. Total metal ion concentration in each step is known and metal ions those didn't bind with **PT-1** will certainly bind with EDTA. So the concertation of Zn-EDTA could be calculated by subtracting the 5th column from the 2nd column. Now, $\{([Peptoid]_{total}/[Zn^{2+}\text{-Peptoid}]) - 1\}$ plotted in X

axis and {([EDTA]$_{total}$/[Zn^{2+}-EDTA]) – 1} was plotted in Y axis. From trend-line option in MS Excel, the straight line was fitted without preset value of intercept. The straight line thus obtained provides the slope that is equal to $K_{d(Zn^{2+}\text{-Peptoid})}K_{a(Zn^{2+}\text{-EDTA})}\alpha_{(EDTA)}$. Here $K_{a(Zn^{2+}\text{-EDTA})}$ and $\alpha_{(EDTA)}$ are known. [5] So $K_{d(Zn^{2+}\text{-Peptoid})}$ could be obtained.

The values are $K_{d(Zn^{2+}\text{-Peptoid})}$ for **PT-1**: 1.85 x 10^{-13} M; $K_{d(Cu^{2+}\text{-Peptoid})}$ for **PT-1**: 2.2 x 10^{-12} M; $K_{d(Zn^{2+}\text{-Peptoid})}$ for **PT-2**: 2.65x 10^{-13} M; $K_{d(Zn^{2+}\text{-Peptoid})}$ for **PT-3**: 4.5x 10^{-13} M.

Table S3. Competition experiment data of **PT-1** and EDTA with Zn^{2+} via UV-Vis analysis in water.

[Peptoid]$_{tot}$ (μM)	[Zn^{2+}]$_{tot}$ (μM)	[EDTA]$_{tot}$ (μM)	Abs of (Peptoid+EDTA)-Zn^{2+}	[Zn-Peptoid] (μM)	[Zn-EDTA] (μM)	{([Peptoid]$_{total}$/[Zn^{2+}-Peptoid]) – 1}	{([EDTA]$_{total}$/[Zn^{2+}-EDTA]) – 1}
26.53	6.657789614	26.53	0.043	1.902654867	4.755134747	12.94367442	4.579232012
26.53	9.98003992	26.53	0.0564	2.495575221	7.484464699	9.630815603	2.544675681
26.53	13.29787234	26.53	0.071	3.14159292	10.15627942	7.444760563	1.612177049
26.53	16.61129568	26.53	0.086	3.805309735	12.80598595	5.971837209	1.071687421
26.53	19.92031873	26.53	0.102	4.513274336	15.40704439	4.878215686	0.72193961
26.53	23.22495023	26.53	0.118	5.221238938	18.00371129	4.081169492	0.473585061
26.53	26.52519894	26.53	0.138	6.10619469	20.41900425	3.344768116	0.299279812

Protein sample preparation

PYK**C**PE**C**GKSFSQKSDLVK**H**QRT**H**TG (Apo-ZFP) was purchased from PSL, GmbH (Heidelberg, Germany) and used without further purification. It was dissolved in NH_4OAc buffer (pH 6.5) (1 mM). The disulfide bonds were reduced using dithiothreitol (DTT). CD (circular dichroism) scans was performed at room temperature at concentration of 100μM in buffer solution. The spectra were obtained by averaging four scans per sample in a fused quartz cell (path length = 0.1 cm), over the 370 to 190 nm region at a step of 1nm (scan rate=1 sec/step). CD scans of Apo-ZF was measured first followed by stoichiometric addition of Zn^{2+} with an aim to make Zn-ZF.[6] The CD of Zn^{2+} added Apo-ZF was measured which is same with Zn-ZF.[7] Chelator (**PT-1**) was added to the prepared Zn-ZF in 1:1 equivalent of Zn^{2+} and CD was measured. In each step along with CD the ESI-MS was also executed which confirms the chelation of Zn^{2+} (Fig. S60-62). Similar experiment was repeated in SBF medium as well. Identical results have been obtained that suggest the ability of the chelator to bind Zn^{2+} from protein domain in biological like medium.

DFT analysis

The peptoid (**PT-1**) was optimized was optimized by DFT-D3 calculations (considering the dispersion correction) at the level of B3-LYP with def2-SVP for every atoms and COSMO for acetonitrile, using Turbomole software package (OS: MACOSX, V 7.3). The coordinates are directly taken from the CIF (CCDC number 1922716, Fig. S1).[8] Bipyridine group was replaced with terpyridine, the terpyridine CIF was taken from CCDC 263509.[9] After optimizing the **PT-1** geometry, the coordinate was taken and metal ions were added with a suggested coordination: (a) terpyridine provides three, (b) picolyl pyridine provides one and (c) acetate provides two for Zn**PT-1** and (d) acetate provides one coordination for Cu**PT-1**. Acetate group was taken from acetic acid CIF (database identifier: ACETAC07, deposition number: 131006). The geometries are optimized at the level of DFT-D4 where def2-TZVP for metal ions [Cu^{2+}/ Zn^{2+}]+ def2SVP (C, H, N, O) were used with COSMO for water.

Figures

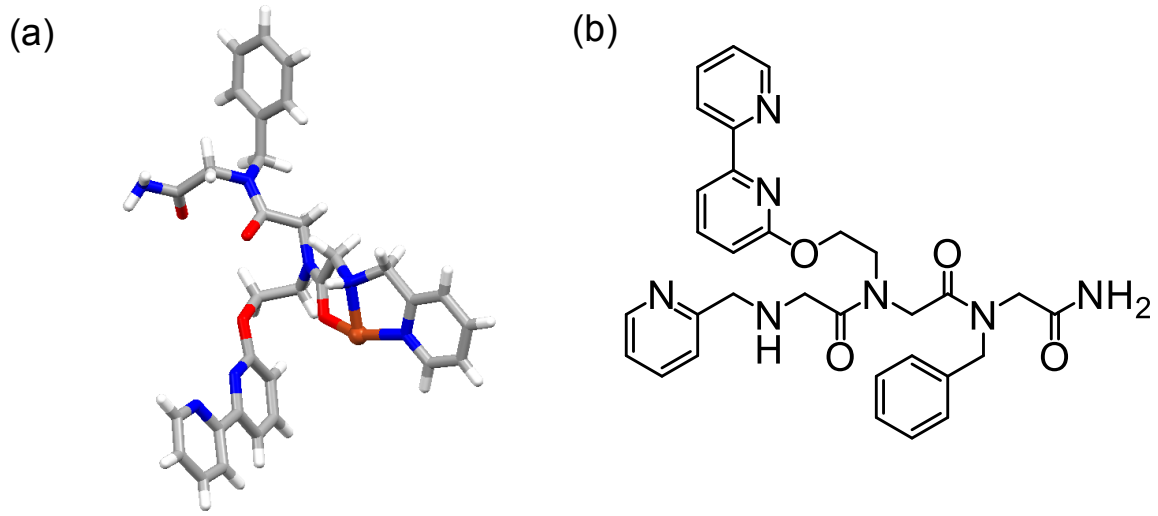

Figure S1. (a) Asymmetric unit of the crystal with CCDC number 1922716[8] (color code: red: oxygen, blue: nitrogen, white: hydrogen, grey: carbon, brown: Cu^{2+}). (b) The chem draw structure of the peptoid in this crystal is shown.

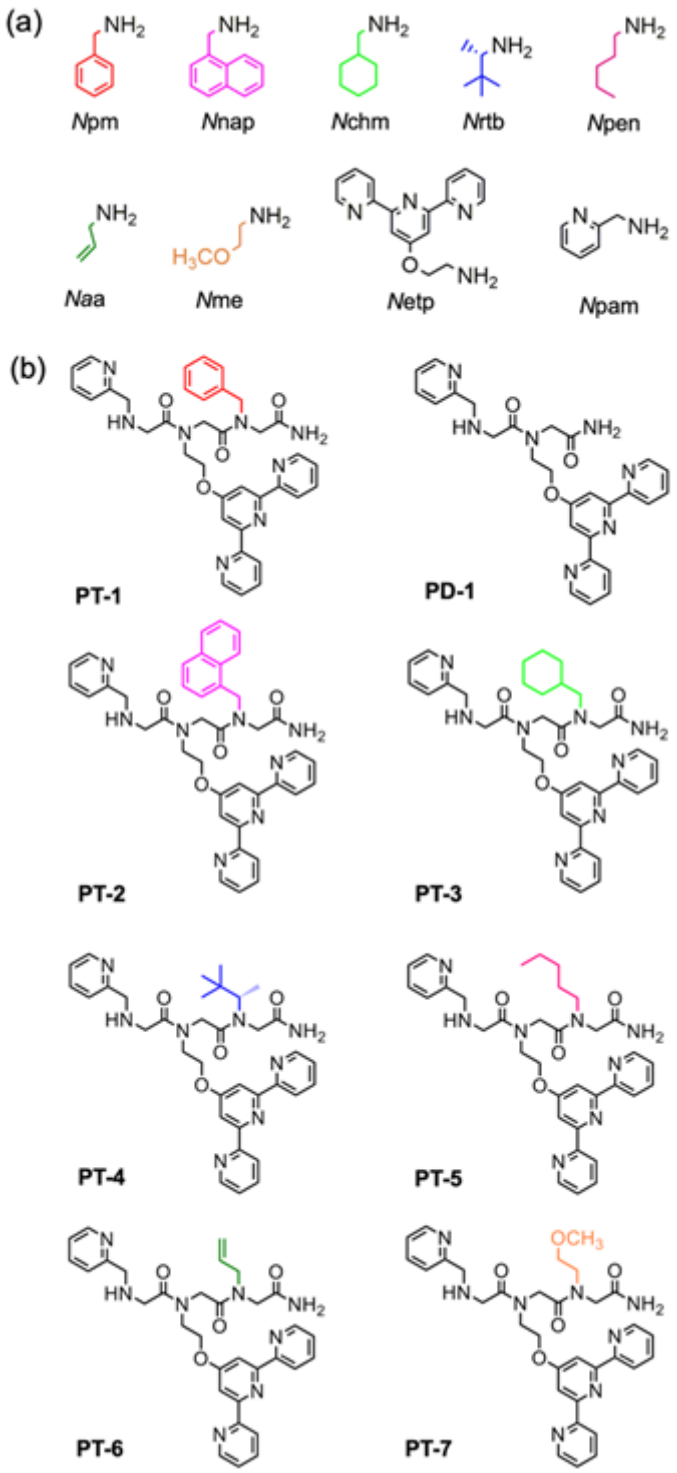

Figure S2. Peptoid oligomers for designing Zn^{2+} chelator; a) achiral and chiral (color choice arbitrary) monomeric units used in the design of the peptoids. b) Chemical sequences of peptoids (**PT-1-7** and **PD-1**) utilised as chelator in this work.

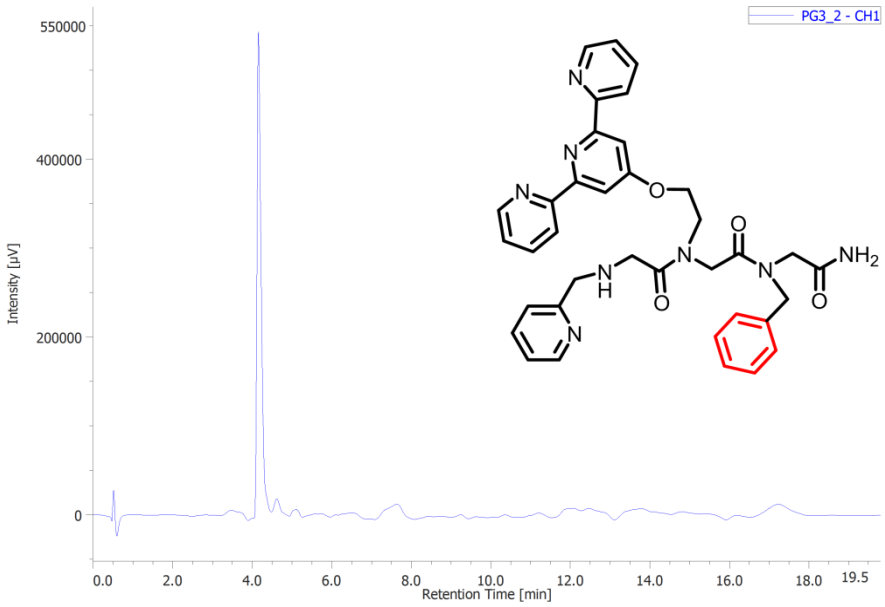

Figure S3. HPLC traces of pure peptoid **PT-1**.

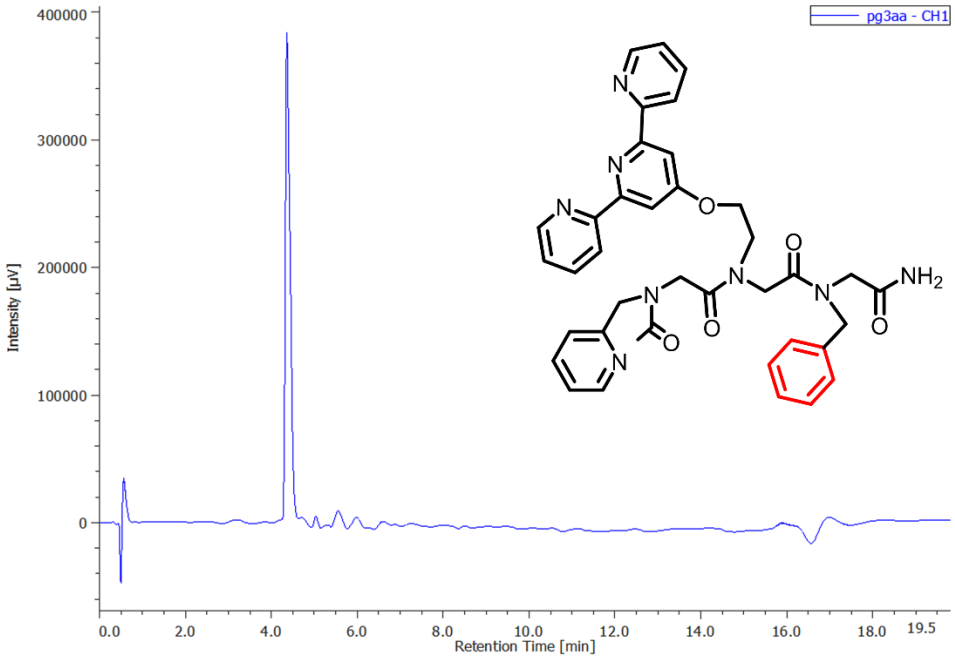

Figure S4. HPLC traces of pure peptoid **PT-1Ac**.

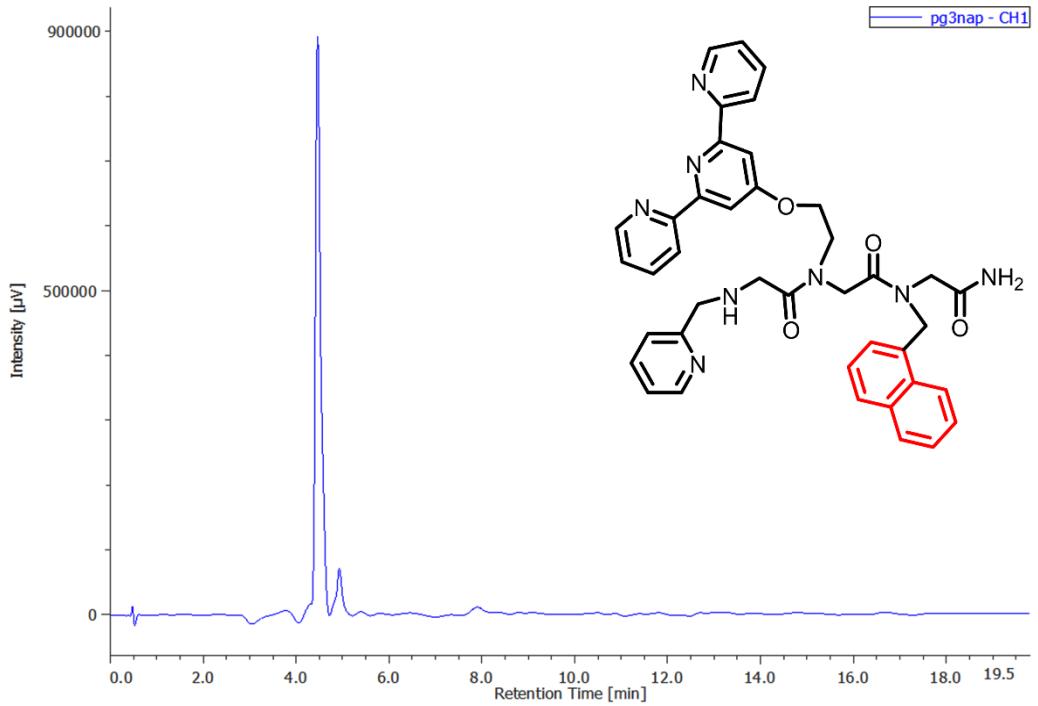

Figure S5. HPLC traces of pure peptoid **PT-2**.

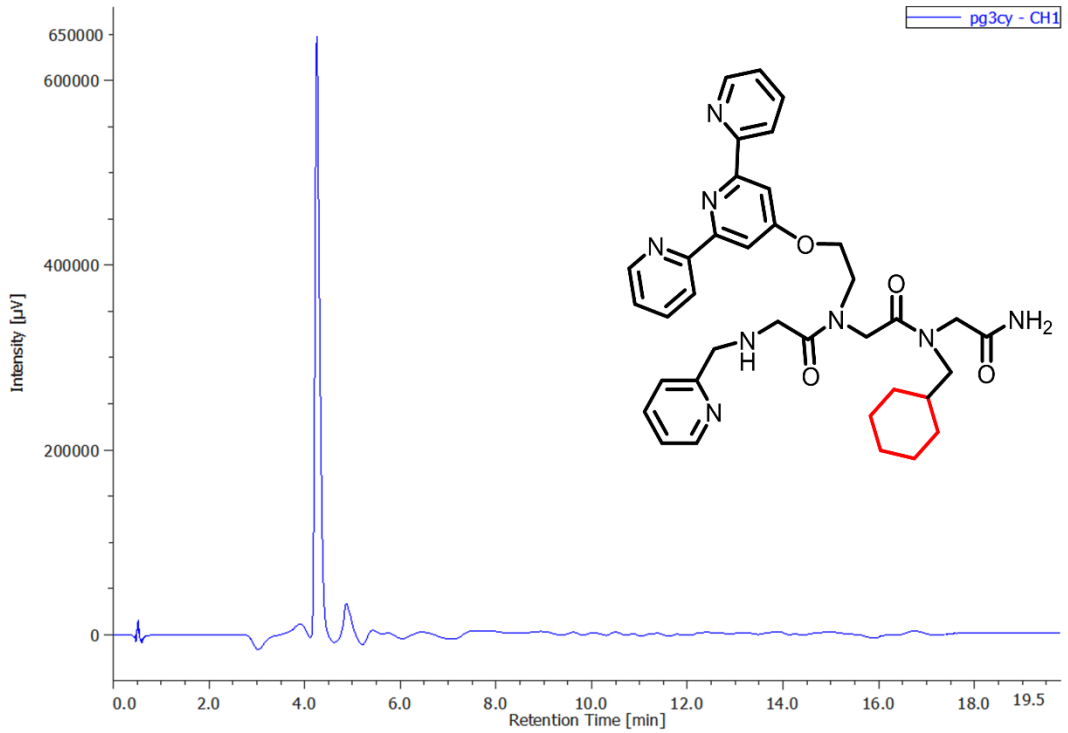

Figure S6. HPLC traces of pure peptoid **PT-3**.

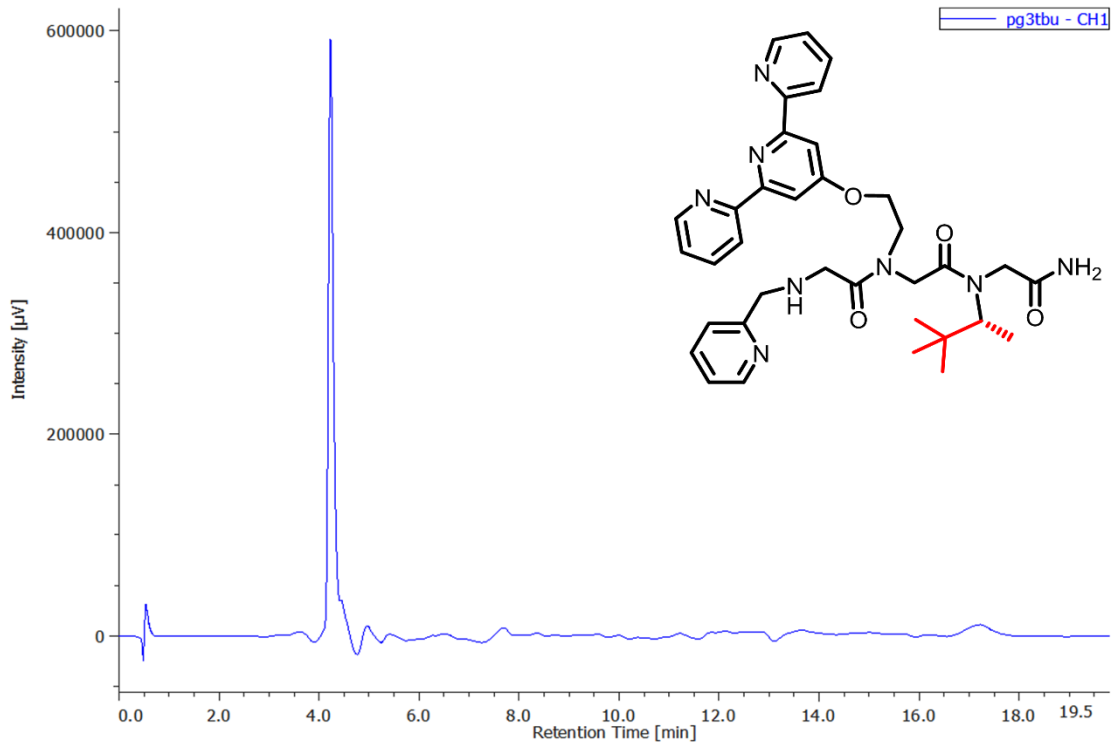

Figure S7. HPLC traces of pure peptoid **PT-4**.

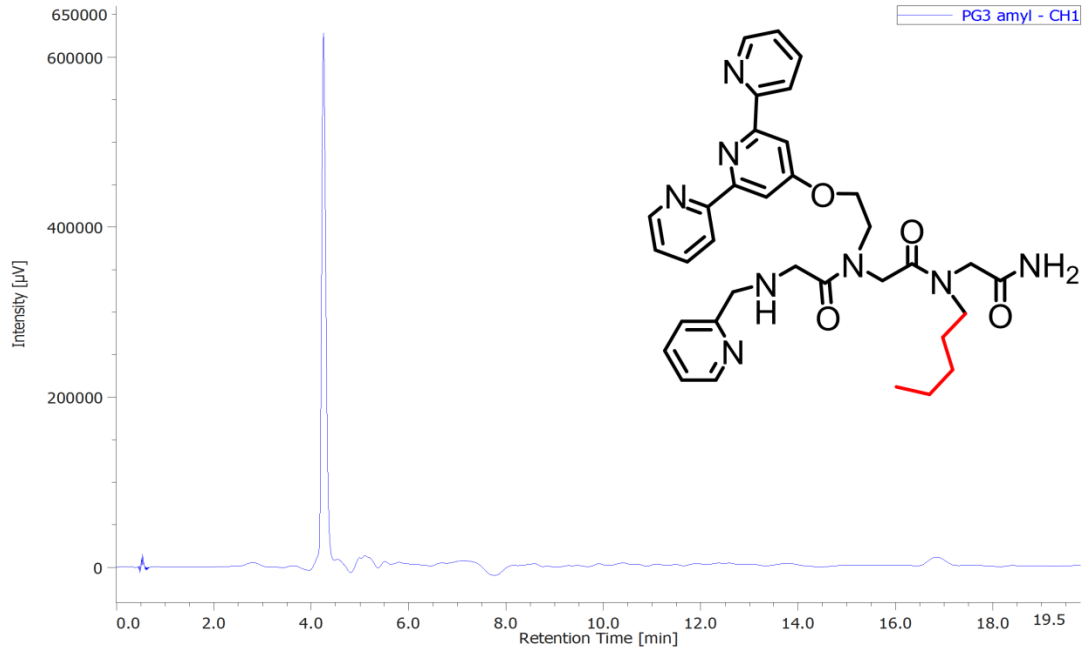

Figure S8. HPLC traces of pure peptoid **PT-5**.

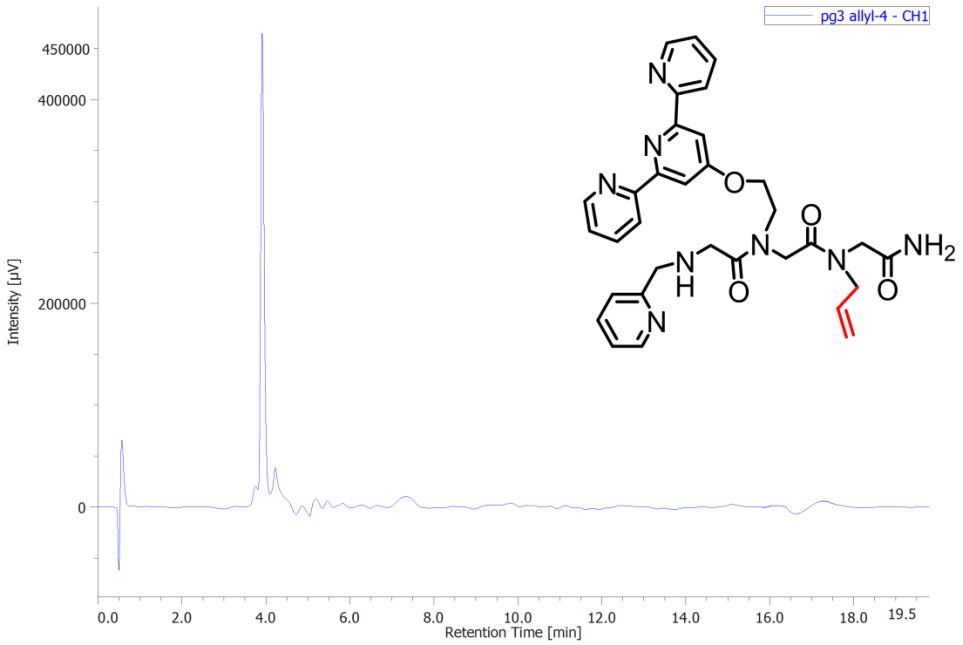

Figure S9. HPLC traces of pure peptoid **PT-6**.

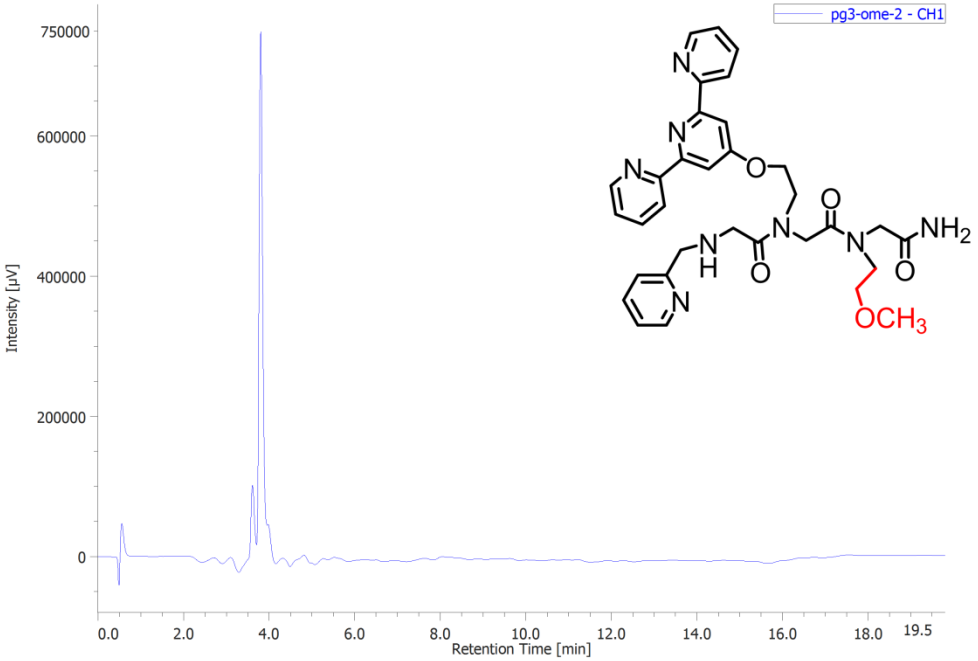

Figure S10. HPLC traces of pure peptoid **PT-7**.

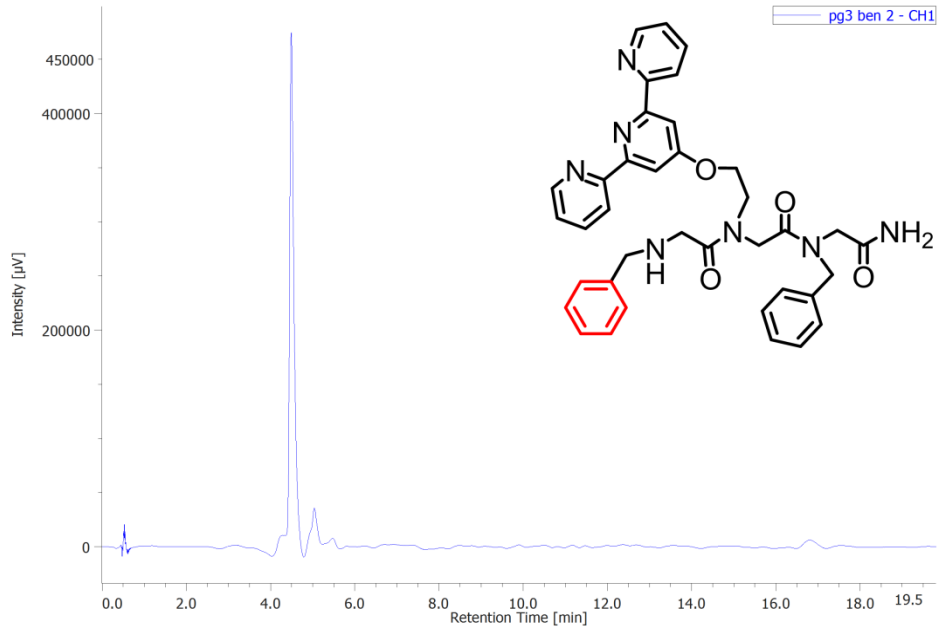

Figure S11. HPLC traces of pure peptoid **PT-8**.

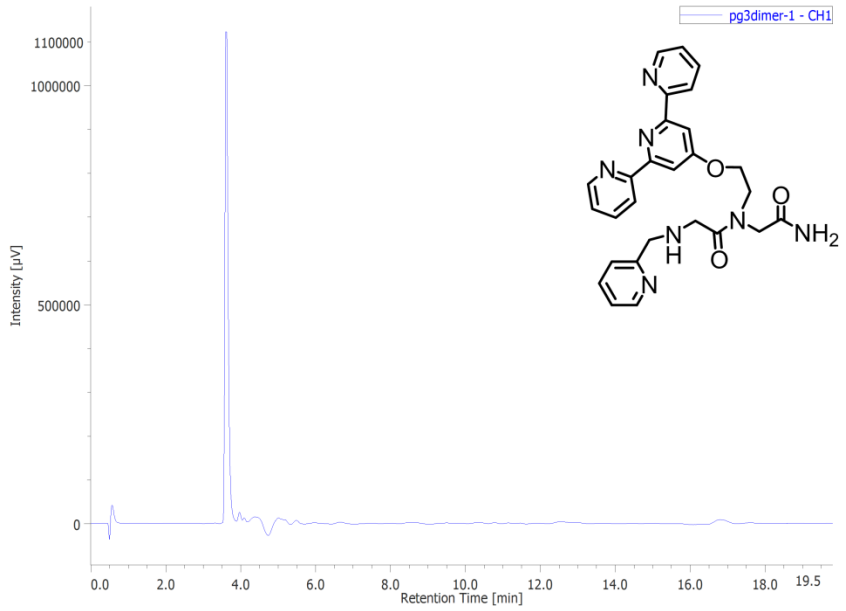

Figure S12. HPLC traces of pure peptoid **PD-1**.

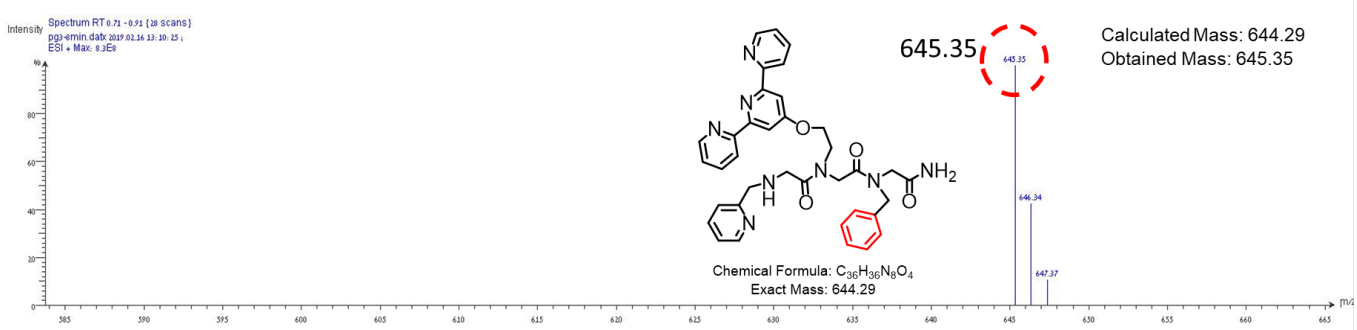

Figure S13. ESI-MS of **PT-1** in water.

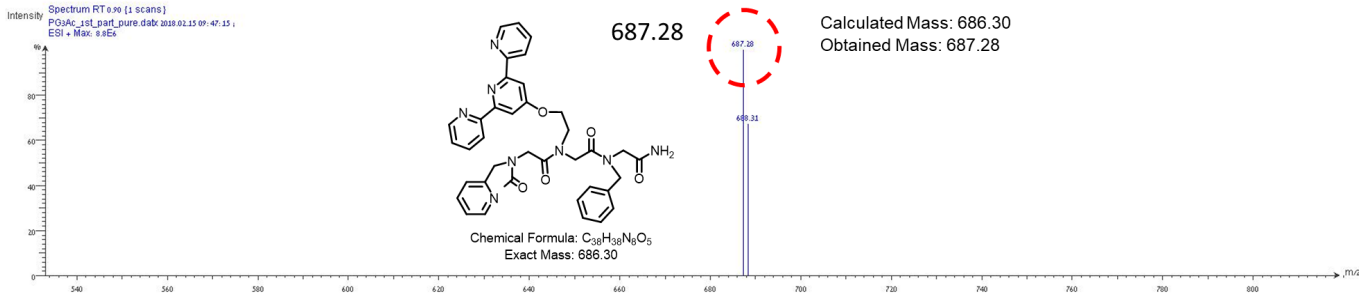

Figure S14. ESI-MS of **PT-1Ac** in water.

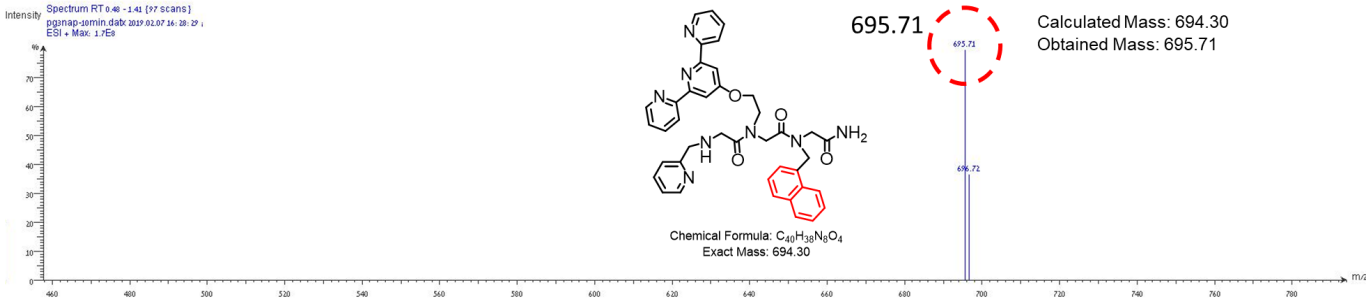

Figure S15. ESI-MS of **PT-2** in water.

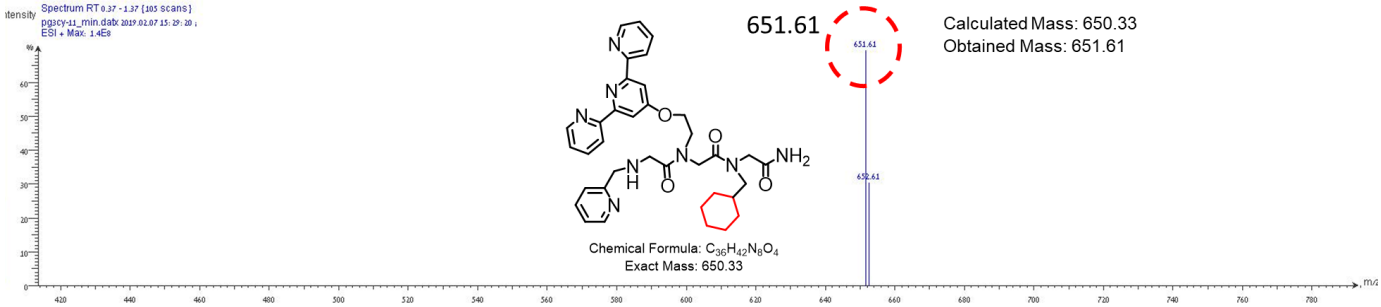

Figure S16. ESI-MS of **PT-3** in water.

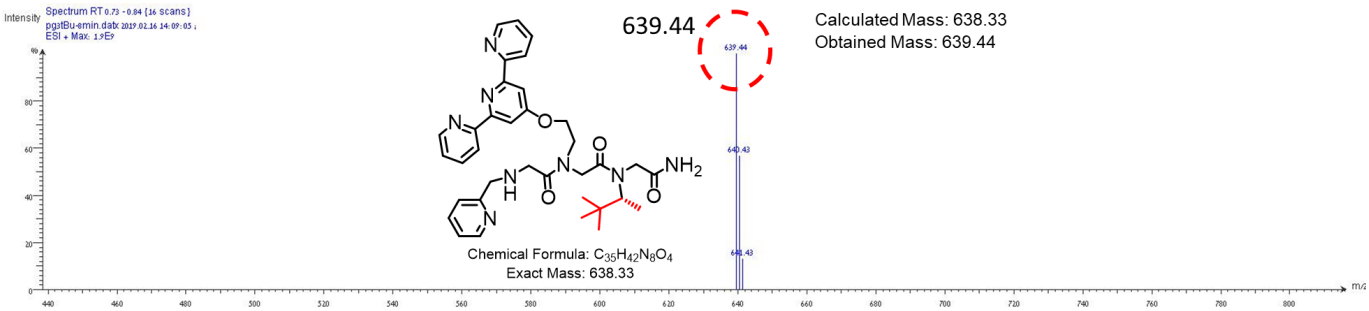

Figure S17. ESI-MS of **PT-4** in water.

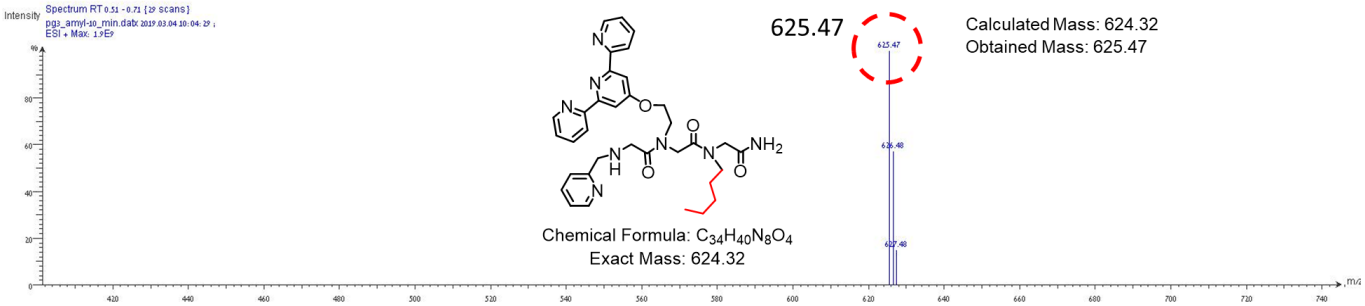

Figure S18. ESI-MS of **PT-5** in water.

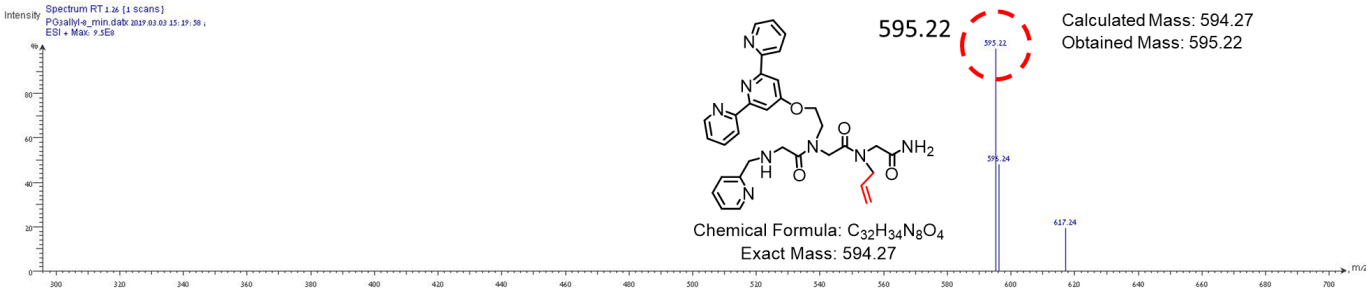

Figure S19. ESI-MS of **PT-6** in water.

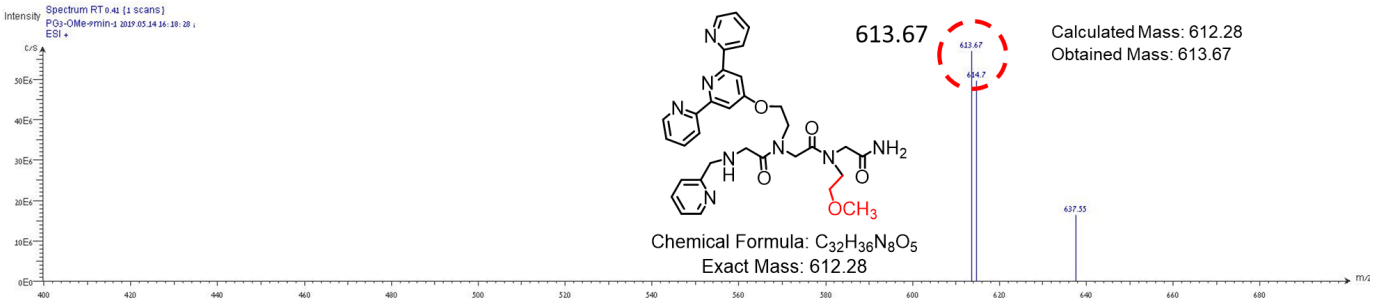

Figure S20. ESI-MS of **PT-7** in water.

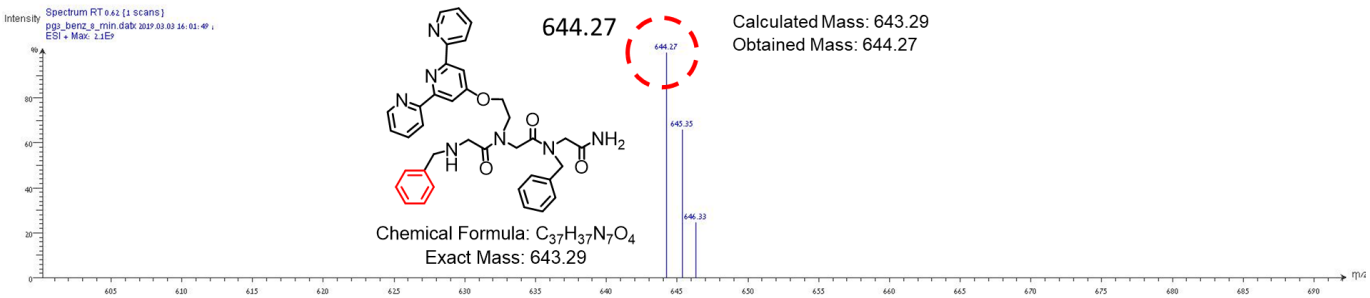

Figure S21. ESI-MS of **PT-8** in water.

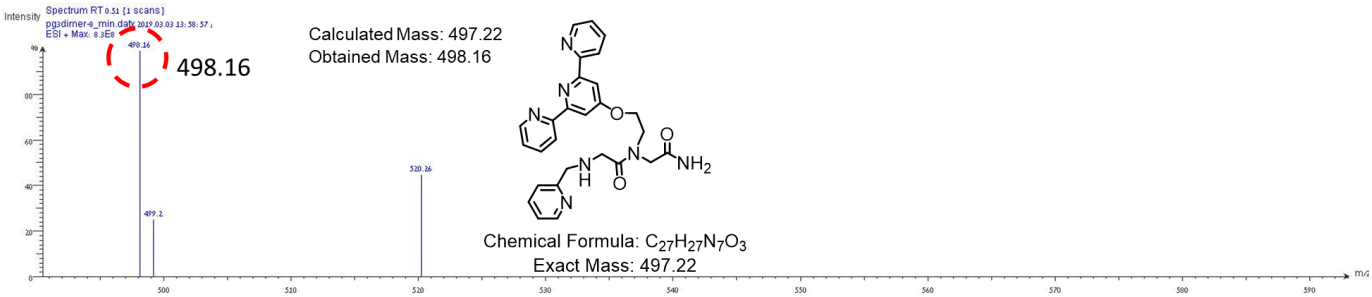

Figure S22. ESI-MS of **PD-1** in water.

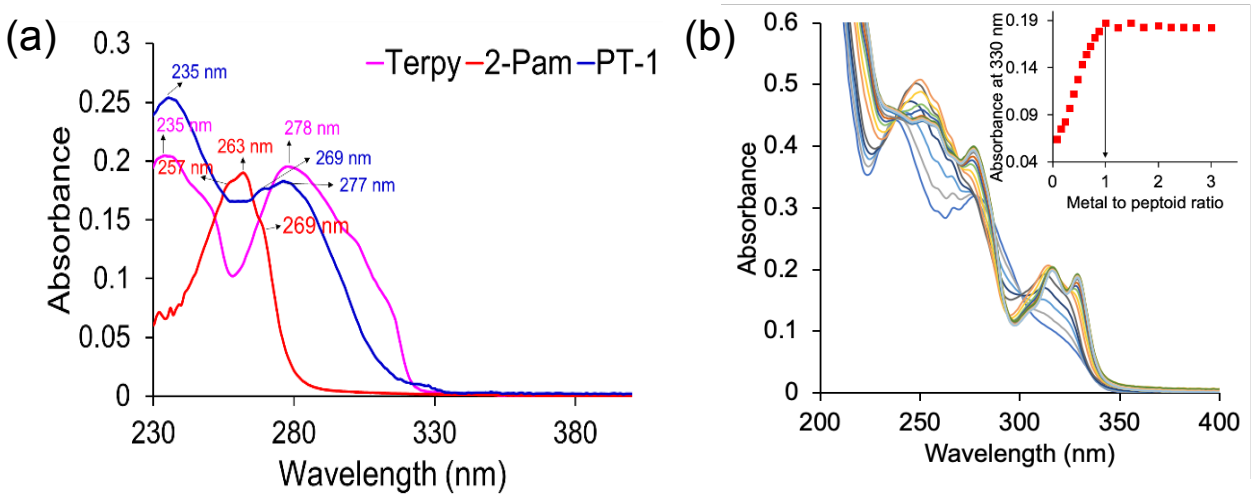

Figure S23. (a) UV-Vis spectrum of Terpyridine (Terpy), 2-picolyl amine (*N*Pam) and **PT-1**, Terpy and *N*Pam are in acetonitrile medium and **PT-1** is in water (8 µM); (b) UV-Vis titration spectra of **PT-1** with Cu^{2+} (17 µM of peptoid, solvent: water titrated with 2µL each time Cu^{2+}, stock solution 2 mM in water).

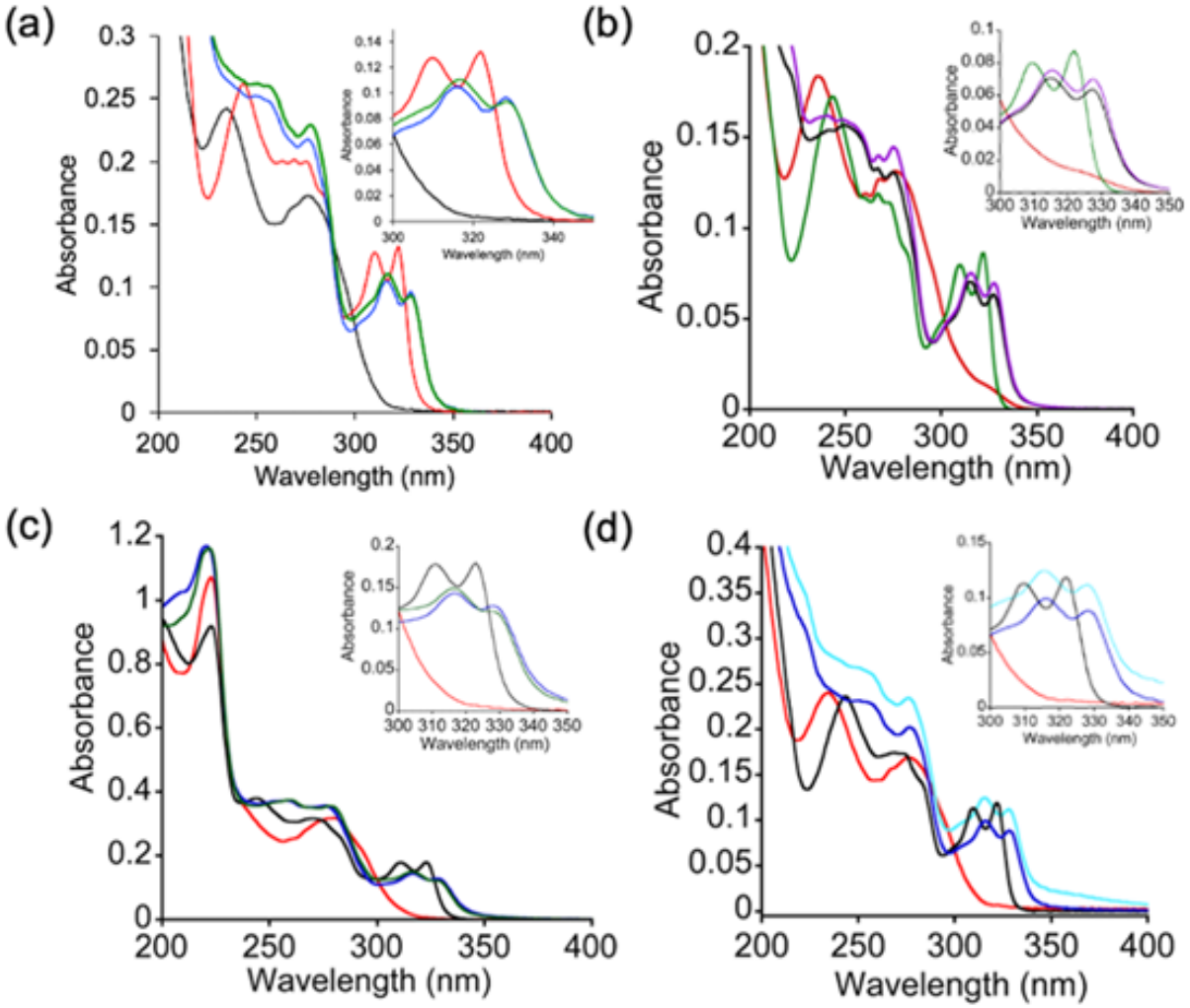

Figure S24. Competition experiment between Zn^{2+} and Cu^{2+} with peptoids (a) **PT-1**; (b) **PD-1**; (c) **PT-2** and (d) **PT-3**; (solvent: water, 8 μM). [For **PT-1** in Fig. a, Black: **PT-1**; Red: Zn**PT-1** Blue: Cu**PT-1** Green: 1:4 (Zn^{2+}:Cu^{2+}). For **PD-1** in Fig. b, Red: **PD-1**; Green: Zn^{2+}- **PD-1**; Black: Cu^{2+}- **PD-1**; Violet: 1:2 (Zn^{2+}:Cu^{2+}). For **PT-2** in Fig. c, Red: **PT-2**; Black: Zn^{2+}- **PT-2**; Blue: Cu^{2+}- **PT-2**; Green: 1:2 (Zn^{2+}:Cu^{2+}). For **PT-3** in Fig. d, Red: **PT-3**; Black: Zn^{2+}- **PT-3**; Blue: Cu^{2+}- **PT-3**; Cyan: 1:2 (Zn^{2+}:Cu^{2+})].

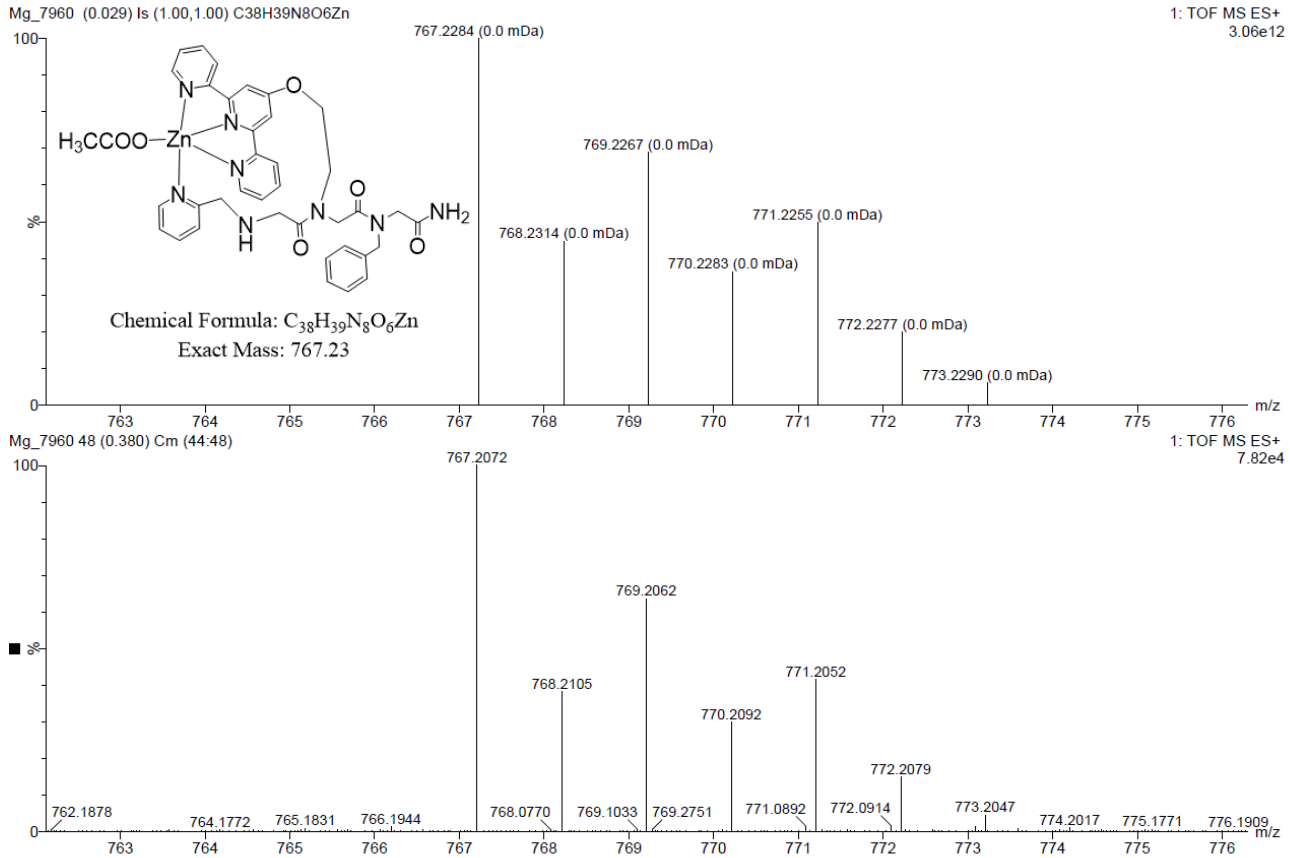

Figure S25. ESI-MS of the aliquot taken from UV-Vis titration of **PT-1** with Zn^{2+}:Cu^{2+} (1:2) in water (8 μM), could be assigned to [(**PT-1**)+Zn^{2+}+OAc^{-}], calculated mass with chemical formula $C_{38}H_{39}N_8O_6Zn$ is 767.23. [Above: Simulated spectrum, below: experimental spectrum].

(a)

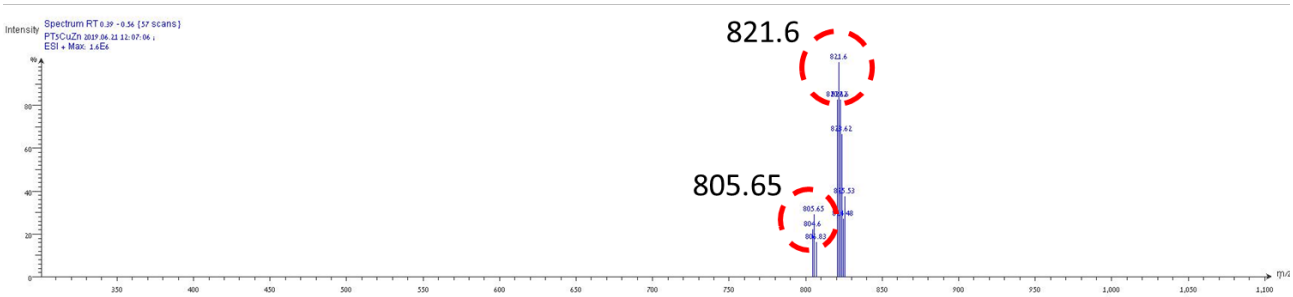

(b)

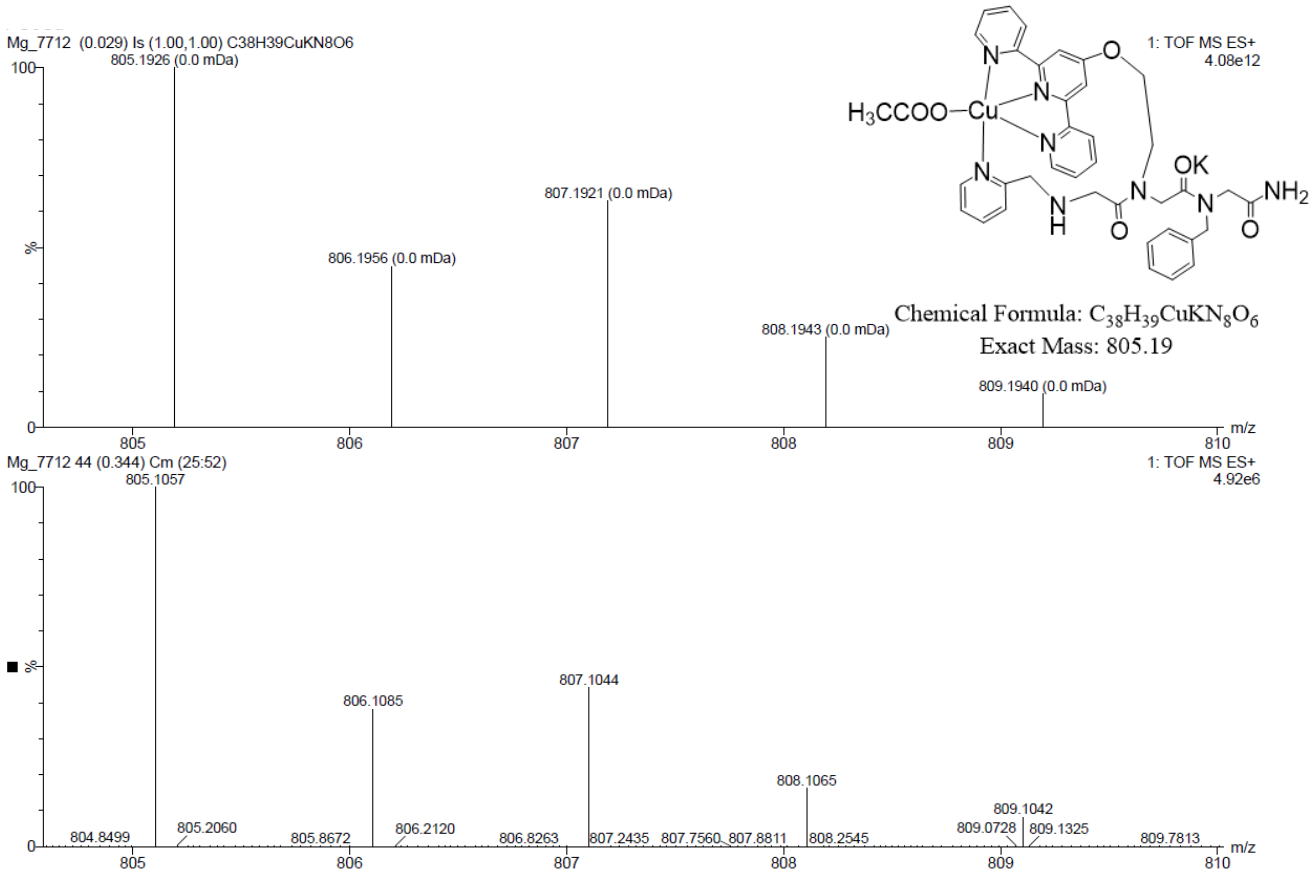

Figure S26. ESI-MS of the aliquot taken from UV-Vis titration of **PT-1** with (a) Zn^{2+}:Cu^{2+} (1:3) {calculated mass for (**PT-1**+Zn^{2+}+OAc^-).3H_2O is 821.26; (**PT-1**+Cu^{2+}+OAc^-+K^+) is 805.19} (b) Zn^{2+}:Cu^{2+} (1:4) in water (8 µM), could be assigned to [(**PT-1**)+Cu^{2+}+OAc^-+K^+] calculated mass is 805.19. [Above: Simulated spectrum, below: experimental spectrum for Fig. S26b].

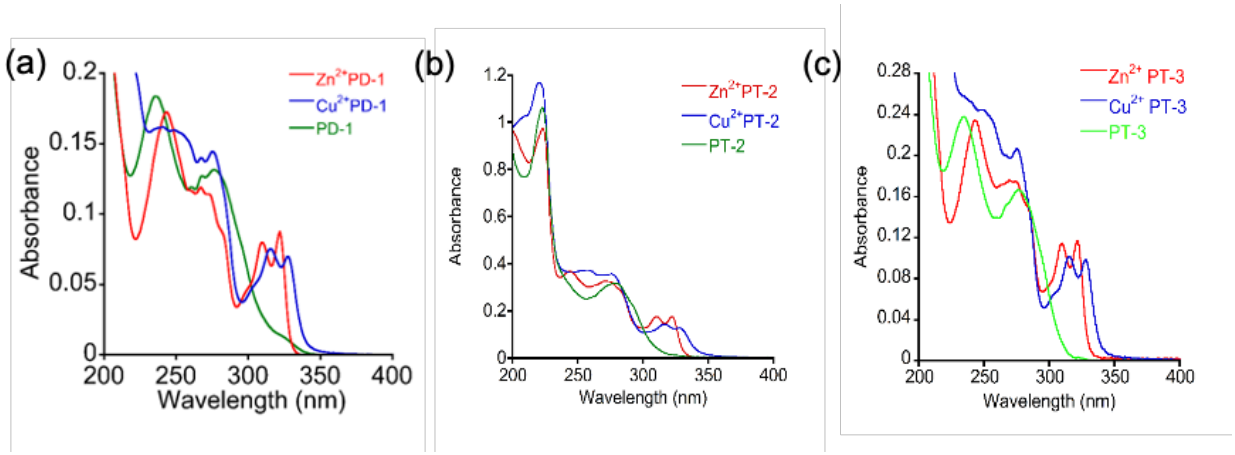

Figure S27. UV-Vis of (a) **PD-1**, (b) **PT-2** and (c) **PT-3** with Cu^{2+} and Zn^{2+} (8 μM, solvent: water).

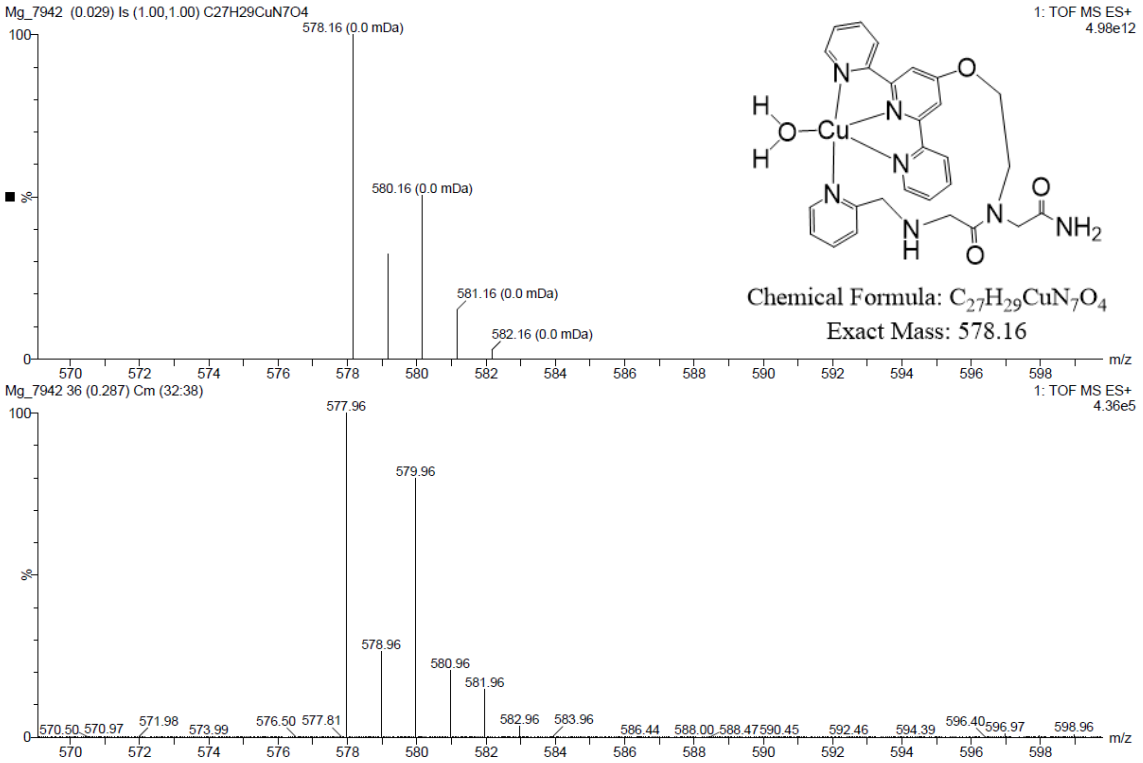

Figure S28. ESI-MS of the aliquot taken from UV-Vis titration of **PD-1** with Zn^{2+}:Cu^{2+} (1:2) in water (8 μM), could be assigned to [(**PD-1**)+Cu^{2+}+(H_2O)]. [Above: Simulated spectrum, below: experimental spectrum].

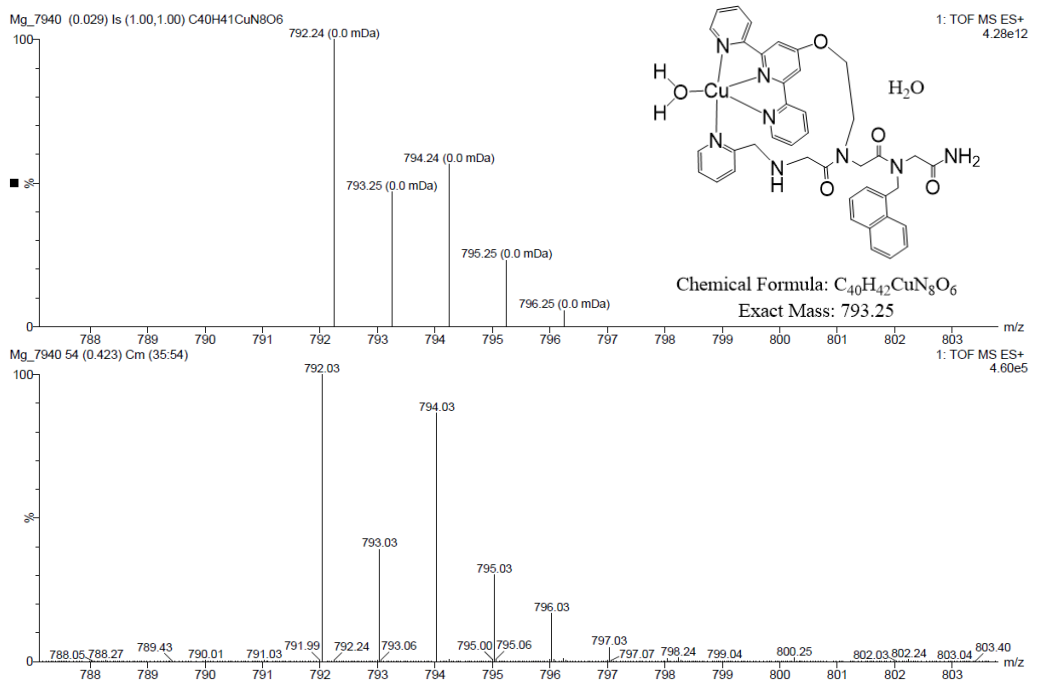

Figure S29. ESI-MS of the aliquot taken from UV-Vis titration of **PT-2** with Zn^{2+}:Cu^{2+} (1:2) in water (8 μM), could be assigned to [(**PT-2**)+Cu^{2+}+H_2O]. H_2O. [Above: Simulated spectrum, below: experimental spectrum].

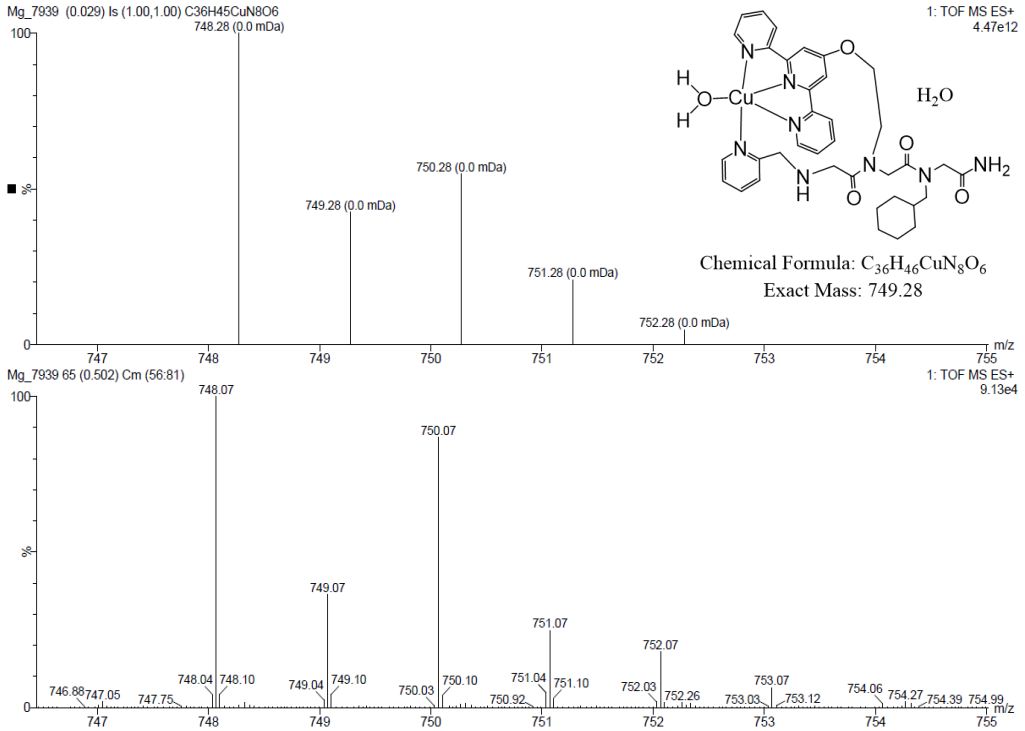

Figure S30. ESI-MS of the aliquot taken from UV-Vis titration of **PT-3** with Zn^{2+}:Cu^{2+} (1:2) in water (8 μM), could be assigned to [(**PT-3**)+Cu^{2+}+H_2O]. H_2O. [Above: Simulated spectrum, below: experimental spectrum].

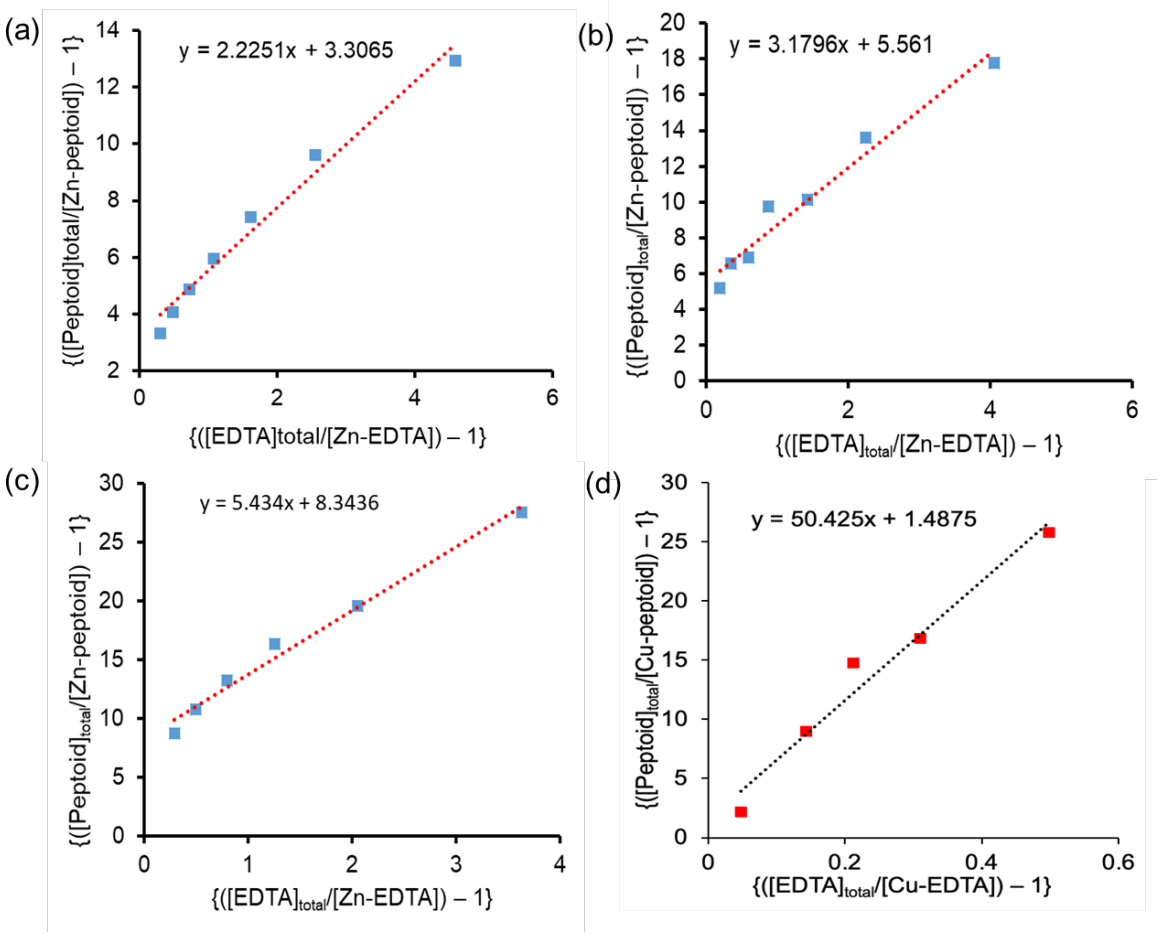

Figure S31. Dissociation constant calculation for (a) **PT-1**, (b) **PT-2**, (c) **PT-3** by competition with EDTA for Zn^{2+} and (d) **PT-1** by competition with EDTA for Cu^{2+} (solvent: water, see experimental section above for details).

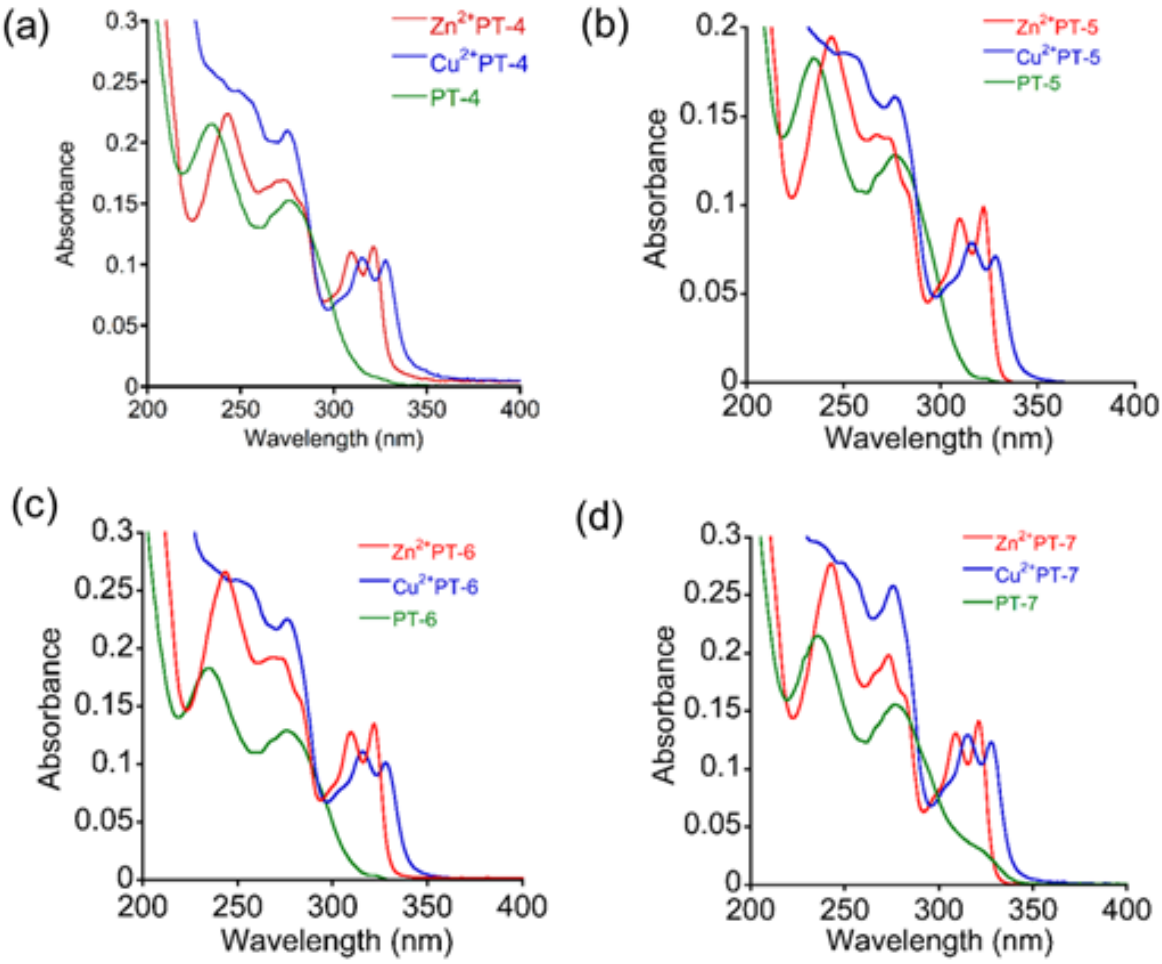

Figure S32. UV-Vis of (a) **PT-4**, (b) **PT-5**, (c) **PT-6**, and (d) **PT**-7 with Cu^{2+} and Zn^{2+} (8 μM, solvent: water).

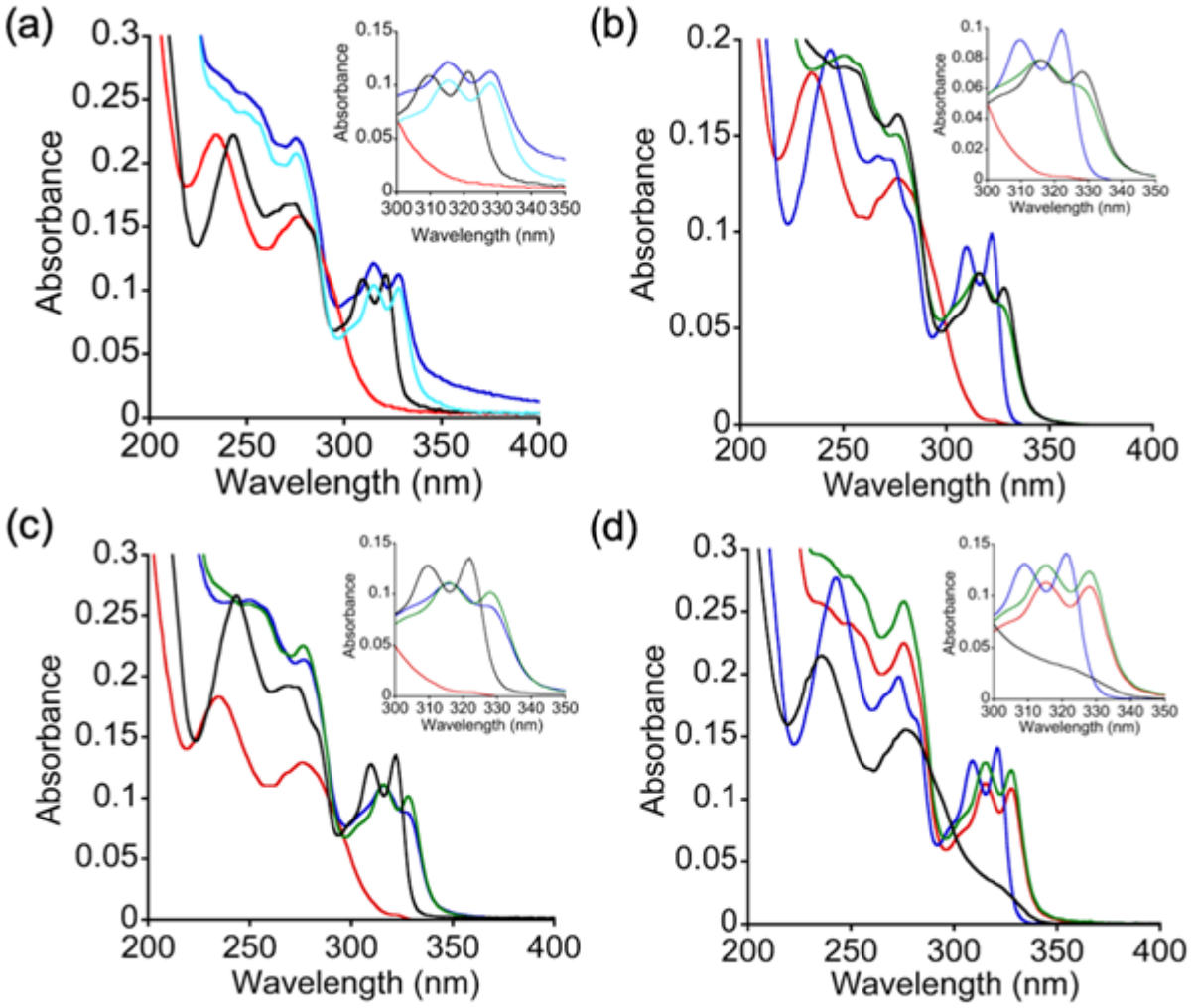

Figure S33. Competition experiment between Zn^{2+} and Cu^{2+} with peptoids (a) **PT-4**; (b) **PT-5**; (c) **PT-6** and (d) **PT-7**; (solvent: water, 8 µM). [For **PT-4** in Fig. a, Red: **PT-4**; Black: Zn^{2+}- **PT-4**; Blue: Cu^{2+}- **PT-4**; Cyan: 1:2 (Zn^{2+}:Cu^{2+}). For **PT-5** in Fig. b, Red: **PT-5**; Blue: Zn^{2+}- **PT-5**; Black: Cu^{2+}- **PT-5**; Green: 1:2 (Zn^{2+}:Cu^{2+}). For **PT-6** in Fig. c, Red: **PT-6**; Black: Zn^{2+}- **PT-6**; Blue: Cu^{2+}- **PT-6**; Green: 1:2 (Zn^{2+}:Cu^{2+}). For **PT-7** in Fig. d, Black: **PT-7**; Blue: Zn^{2+}- **PT-7**; Red: Cu^{2+}- **PT-7**; Green: 1:2 (Zn^{2+}:Cu^{2+})].

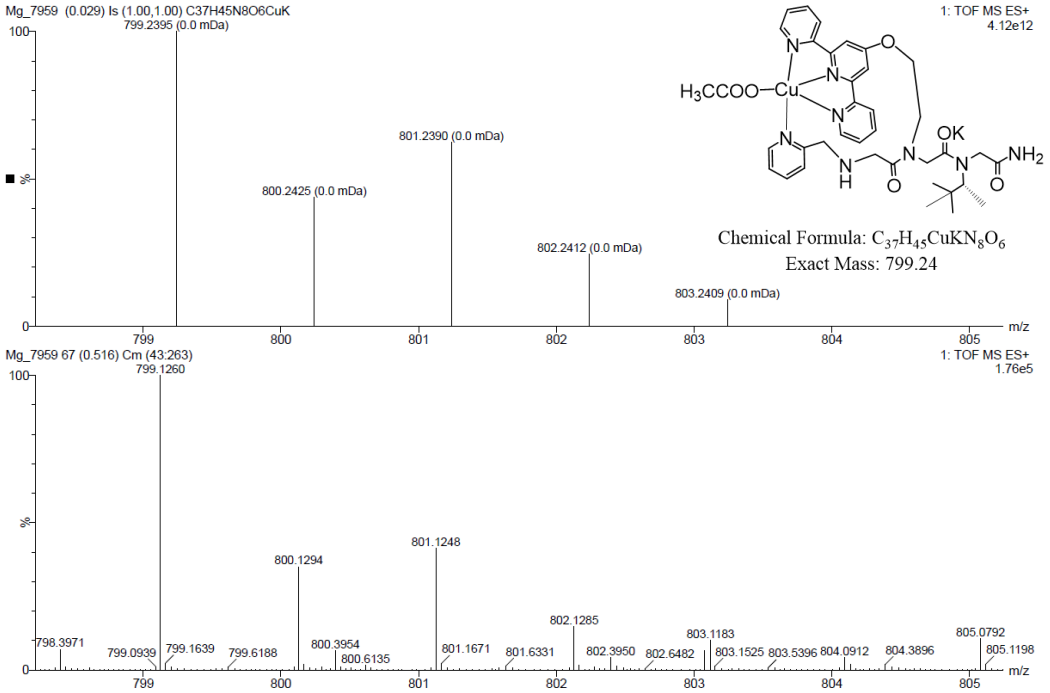

Figure S34. ESI-MS of the aliquot taken from UV-Vis titration of **PT-4** with Zn^{2+}:Cu^{2+} (1:2) in water (8 μM), could be assigned to [(**PT-4**)+Cu^{2+}+(OAc^{-})+K^{+}]. [Above: Simulated spectrum, below: experimental spectrum].

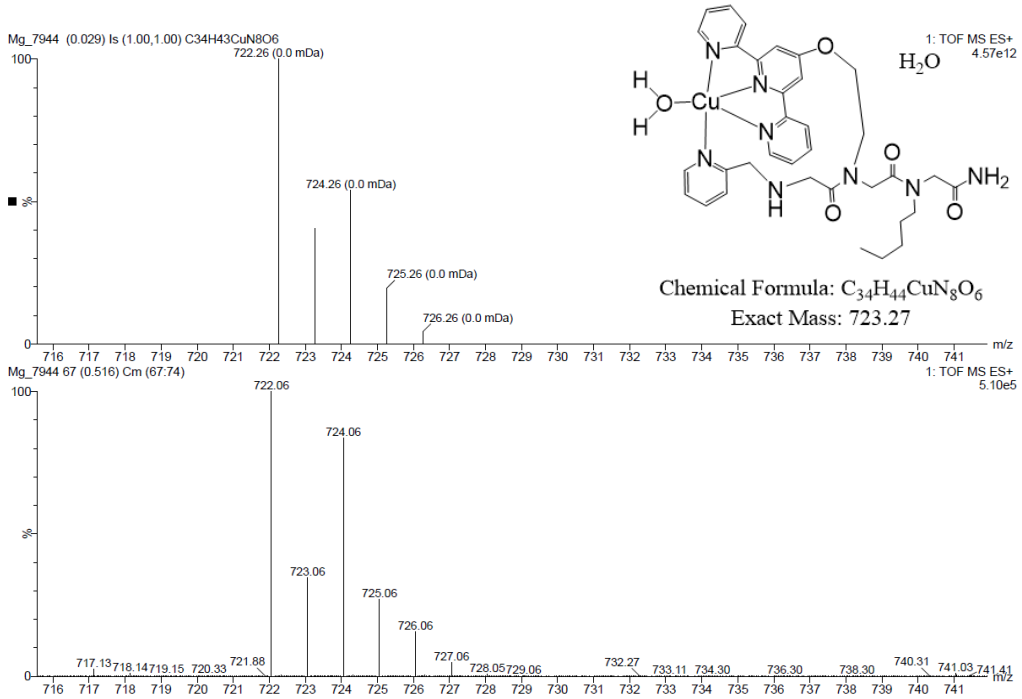

Figure S35. ESI-MS of the aliquot taken from UV-Vis titration of **PT-5** with Zn^{2+}:Cu^{2+} (1:2) in water (8 μM), could be assigned to [(**PT-5**)+Cu^{2+}+H_2O]. H_2O. [Above: Simulated spectrum, below: experimental spectrum].

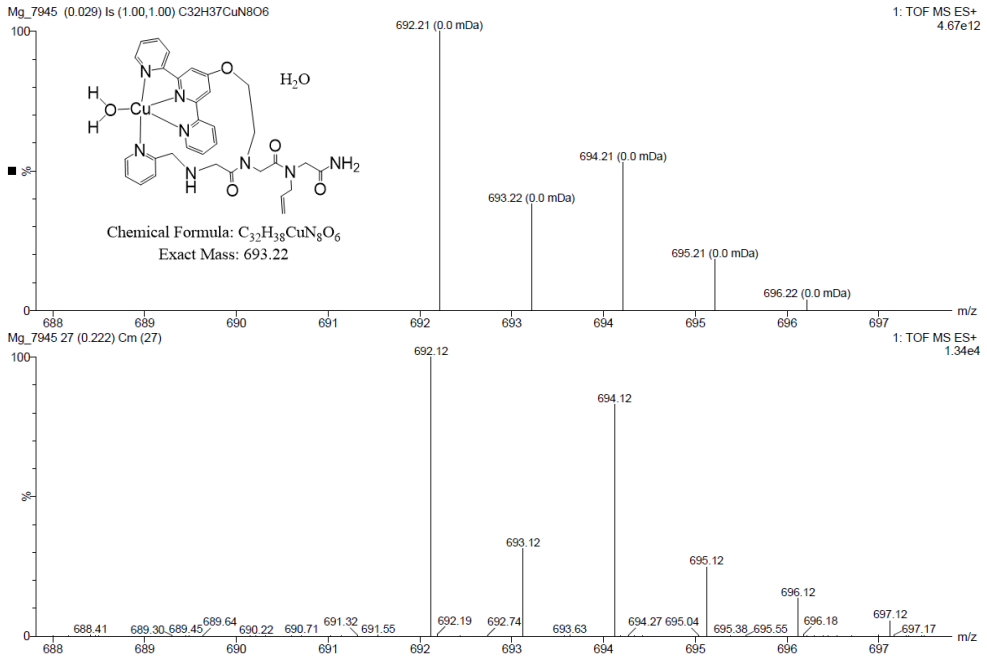

Figure S36. ESI-MS of the aliquot taken from UV-Vis titration of **PT-6** with Zn^{2+}:Cu^{2+} (1:2) in water (8 μM), could be assigned to [(**PT-6**)+Cu^{2+}+H_2O].H_2O. [Above: Simulated spectrum, below: experimental spectrum].

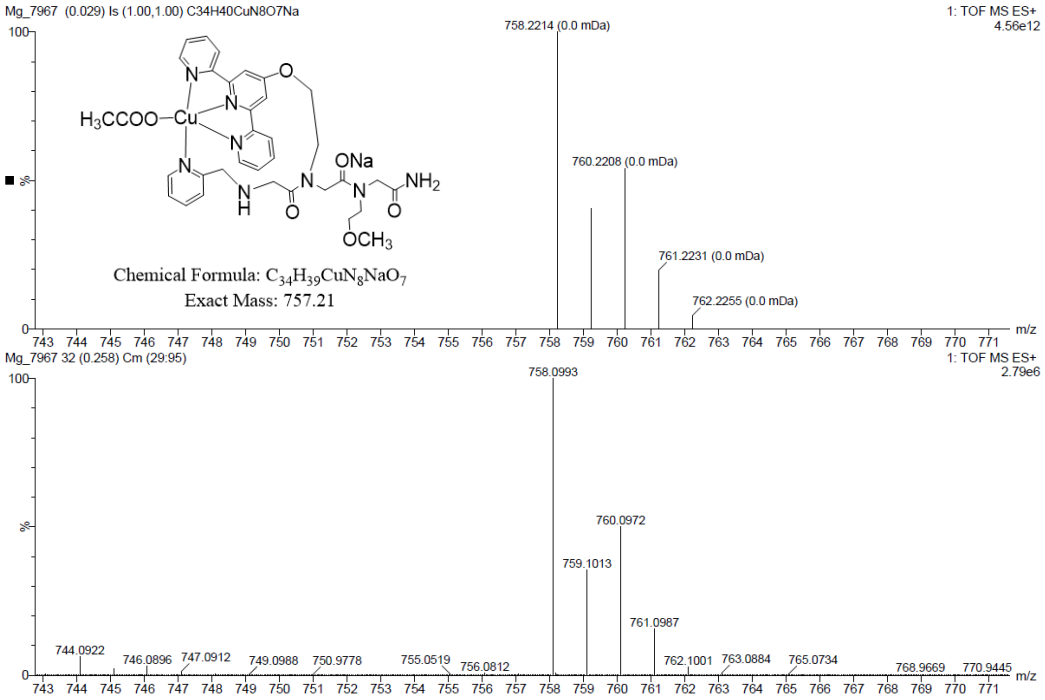

Figure S37. ESI-MS of the aliquot taken from UV-Vis titration of **PT-7** with Zn^{2+}:Cu^{2+} (1:2) in water (8 μM), could be assigned to [(**PT-7**)+Cu^{2+}+OAc^-+Na^+]. [Above: Simulated spectrum, below: experimental spectrum].

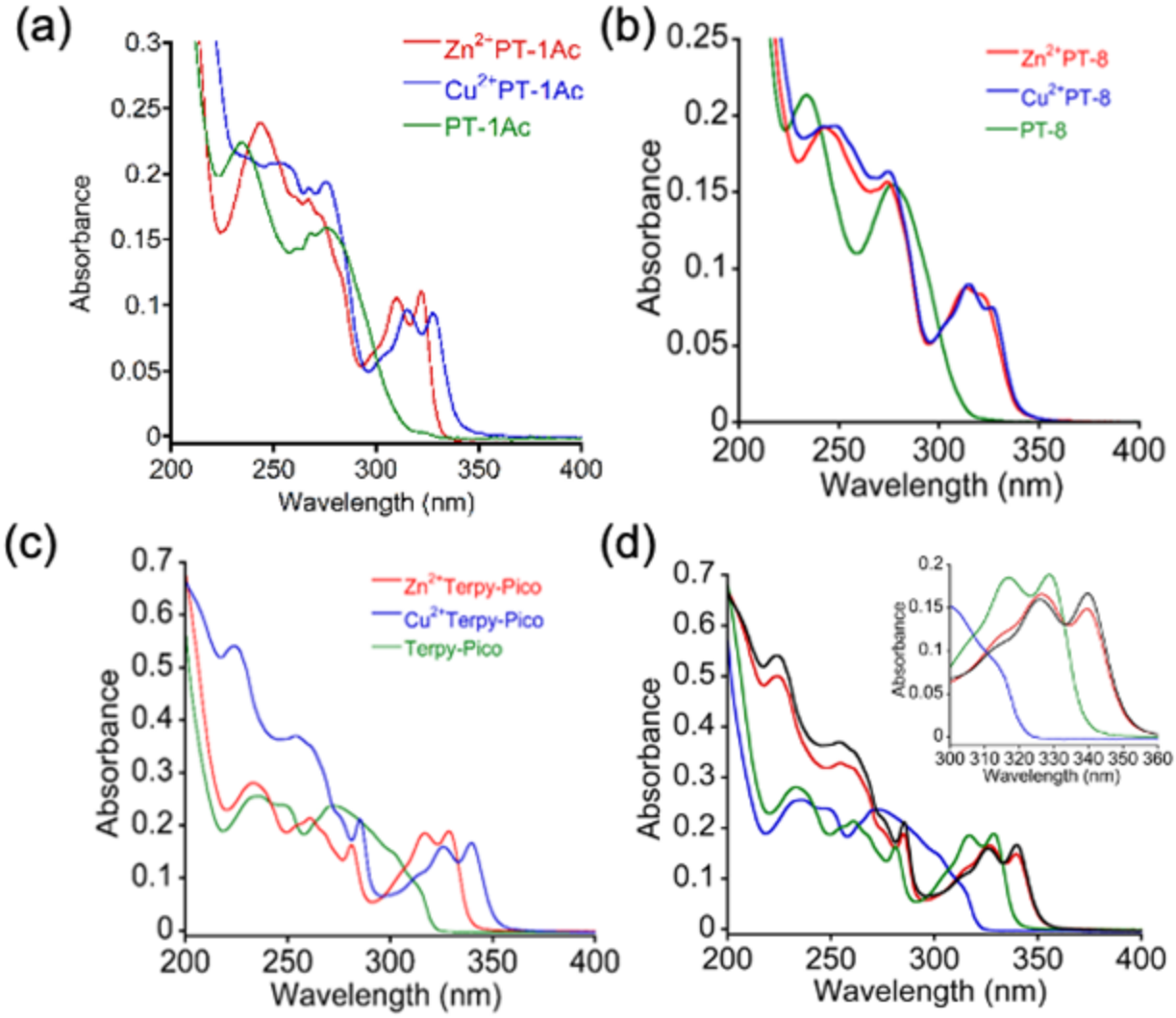

Figure S38. UV-Vis spectra of (a) **PT-1Ac**, (b) **PT-8** and (c) **Terpy** and ***N*pam** mixture with Cu^{2+}(blue) and Zn^{2+}(red); (d) competition experiment between Zn^{2+} and Cu^{2+} with **Terpy** and ***N*pam** (8 μM, solvent: water for a-b and acetonitrile for c-d).

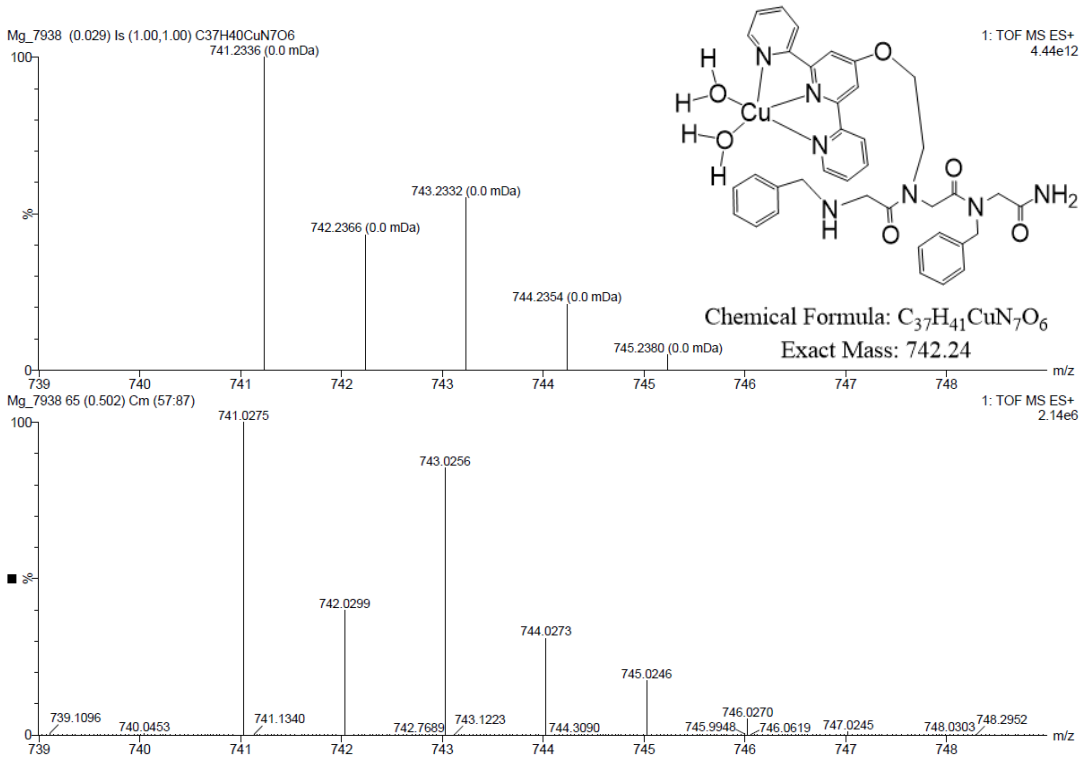

Figure S39. ESI-MS of the aliquot taken from UV-Vis titration of **PT-8** with Zn^{2+}:Cu^{2+} (1:2) in water (8 μM), could be assigned to [(**PT-8**)+Cu^{2+}+$(H_2O)_2$]. [Top: simulated, bottom: experimental spectrum].

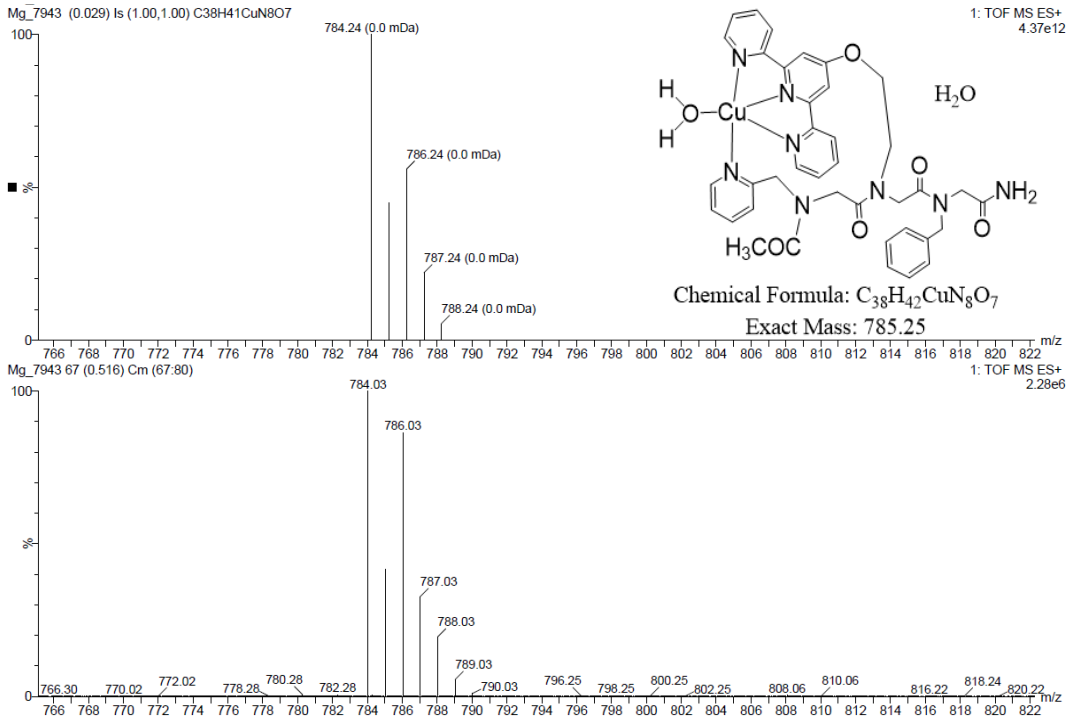

Figure S40. ESI-MS of the aliquot taken from UV-Vis titration of **PT-1Ac** with Zn^{2+}:Cu^{2+} (1:2) in water

(8 μM), could be assigned to [(**PT-1Ac**)+Cu^{2+}+H_2O].H_2O. [Top: simulated spectrum, below: experimental spectrum].

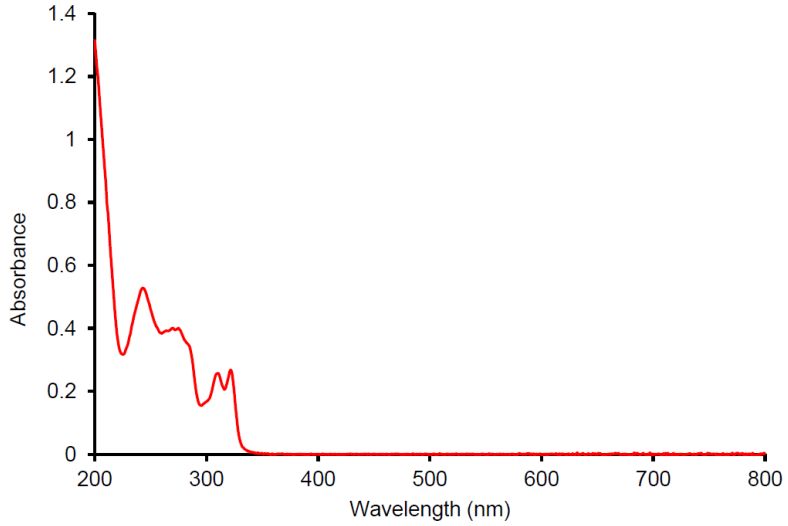

Figure S41. UV-Vis spectrum of Zn**PT-1** complex in water (17 μM).

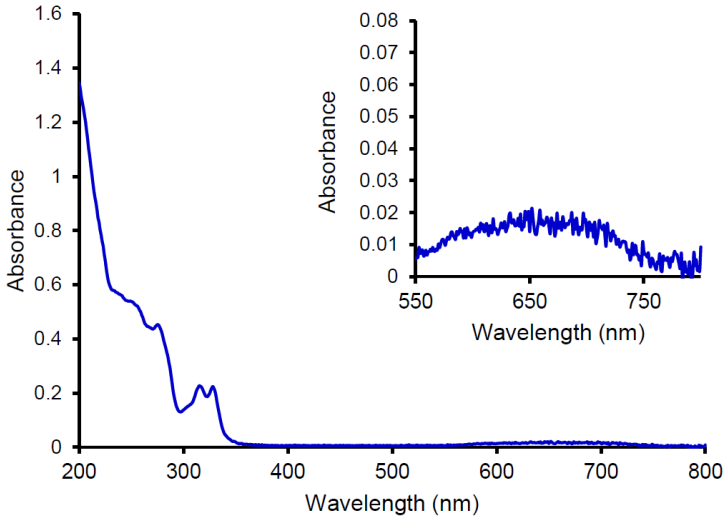

Figure S42. UV-Vis spectrum of Cu**PT-1** complex in water (17 μM), inset shows d-d transition.

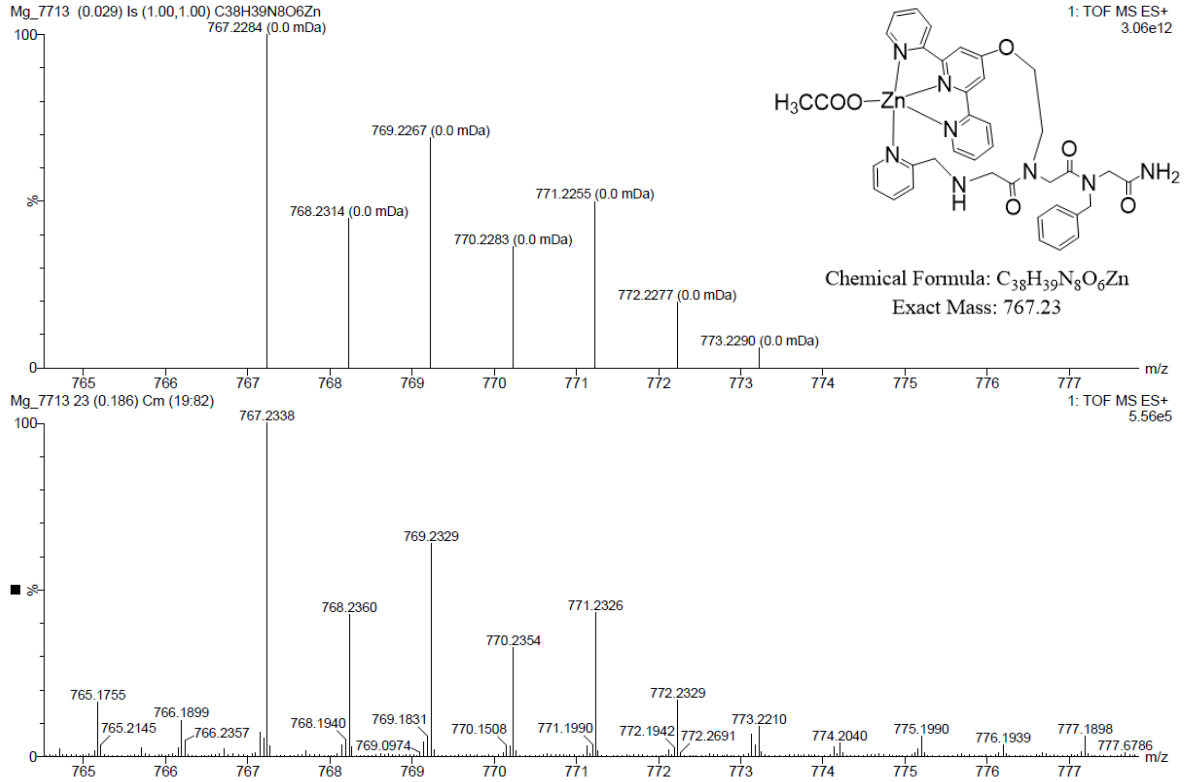

Figure S43. ESI-MS of Zn**PT-1** complex in water, could be assigned to [(**PT-1**)+Zn^{2+}+(OAc^-)]. [Top: Simulated spectrum, bottom: experimental spectrum].

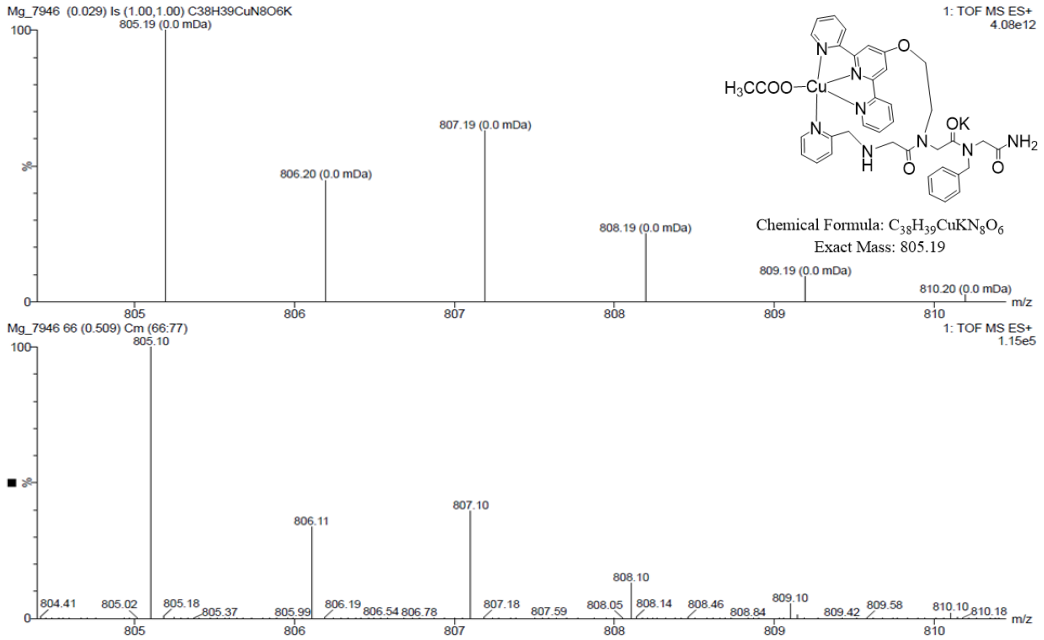

Figure S44. ESI-MS of Cu**PT-1** complex in water, could be assigned to [(**PT-1**)+Cu^{2+}+OAc^-+K^+]. [Top: Simulated spectrum, below: experimental spectrum].

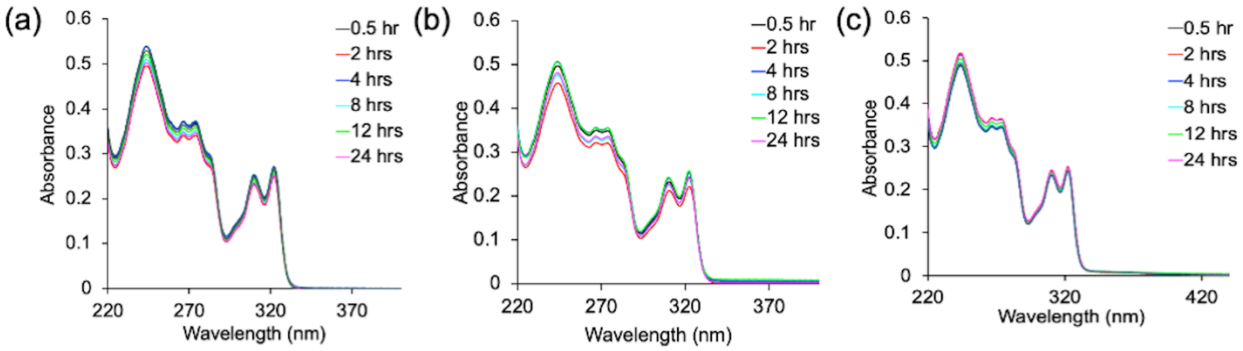

Figure S45. UV-Vis spectrum of Zn**PT-1** complex synthesis in water (a) room temperature, (b) 35°C and (c) 50°C (17 µM).

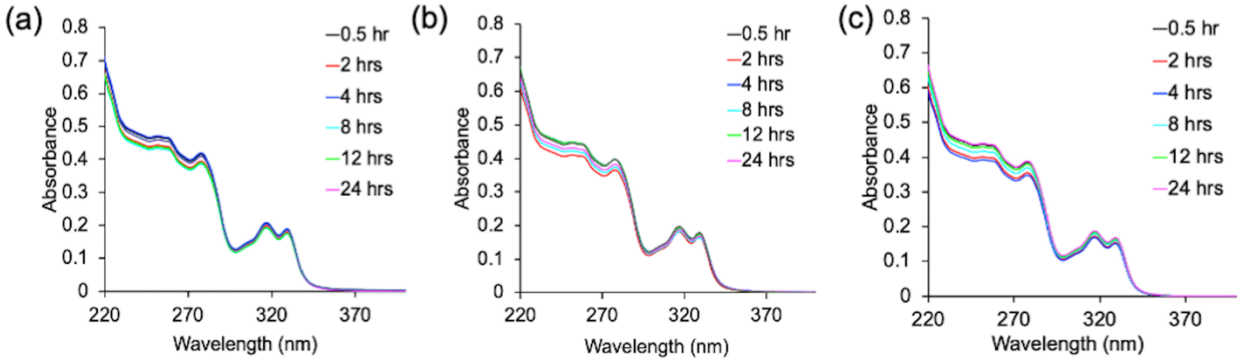

Figure S46. UV-Vis spectrum of Cu**PT-1** complex synthesis in water (a) room temperature, (b) 35°C and (c) 50°C (17 µM).

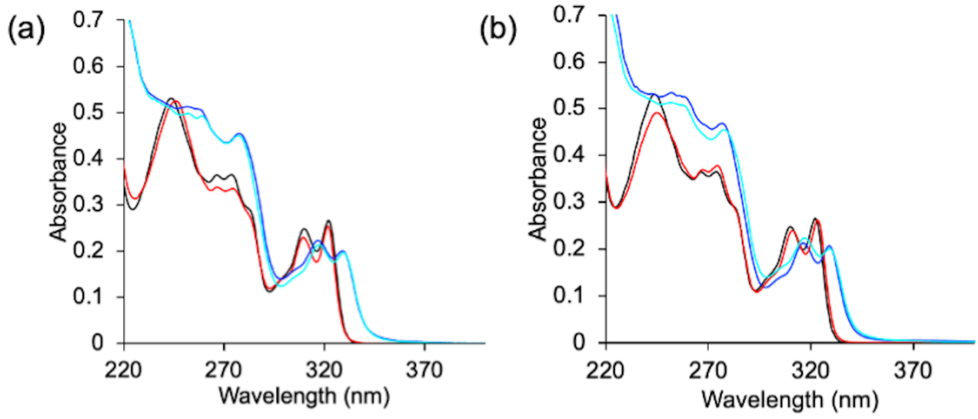

Figure S47. UV-Vis spectrum of Zn^{2+}/Cu^{2+}**PT-1** complex in (a) acetonitrile and (b) methanol (17 µM); [black: Zn**PT-1** complex in water, red: Zn**PT-1** complex in acetonitrile/methanol, blue: Cu**PT-1** complex in water, cyan: Cu**PT-1** complex in acetonitrile/methanol].

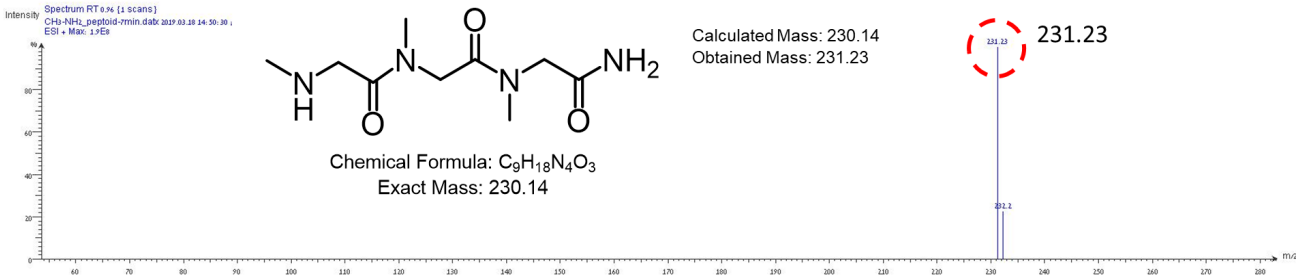

Figure S48. ESI-MS of **PT-9** in acetonitrile.

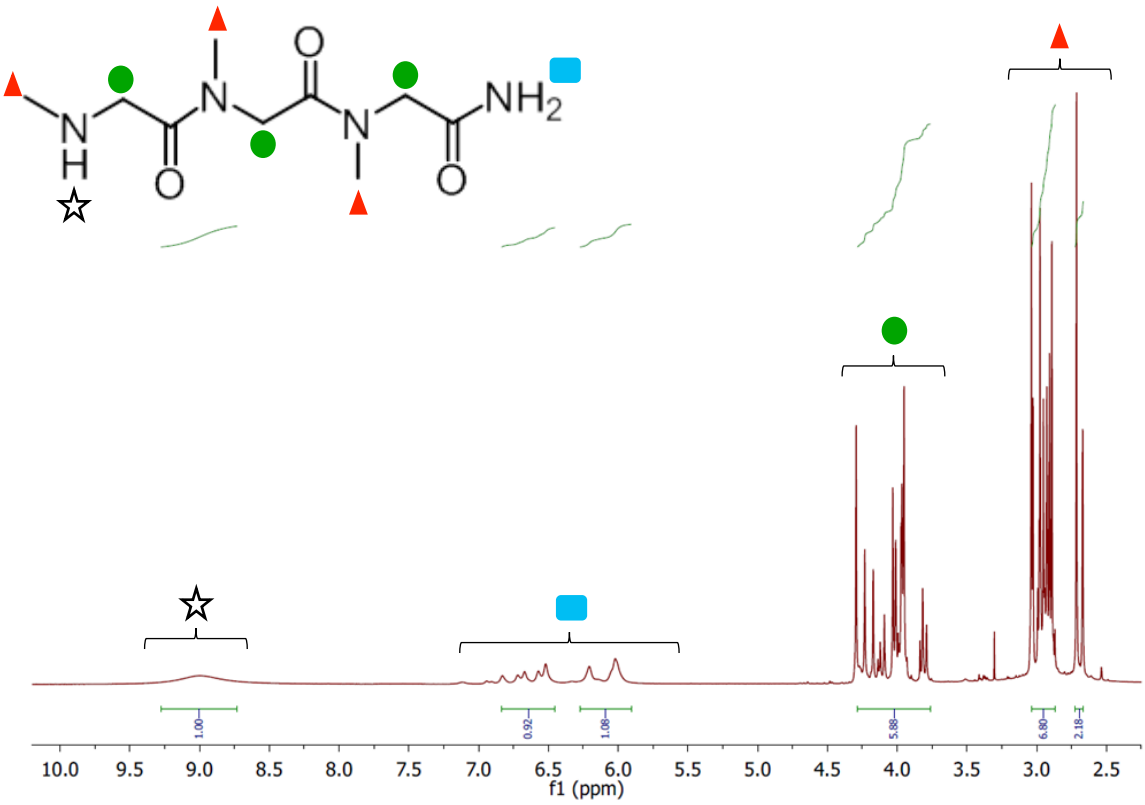

Figure S49. ^{1}H-NMR (in 400MHz) chemical shift of **PT-9** ($C_9H_{18}N_4O_3$) in CD_3CN.

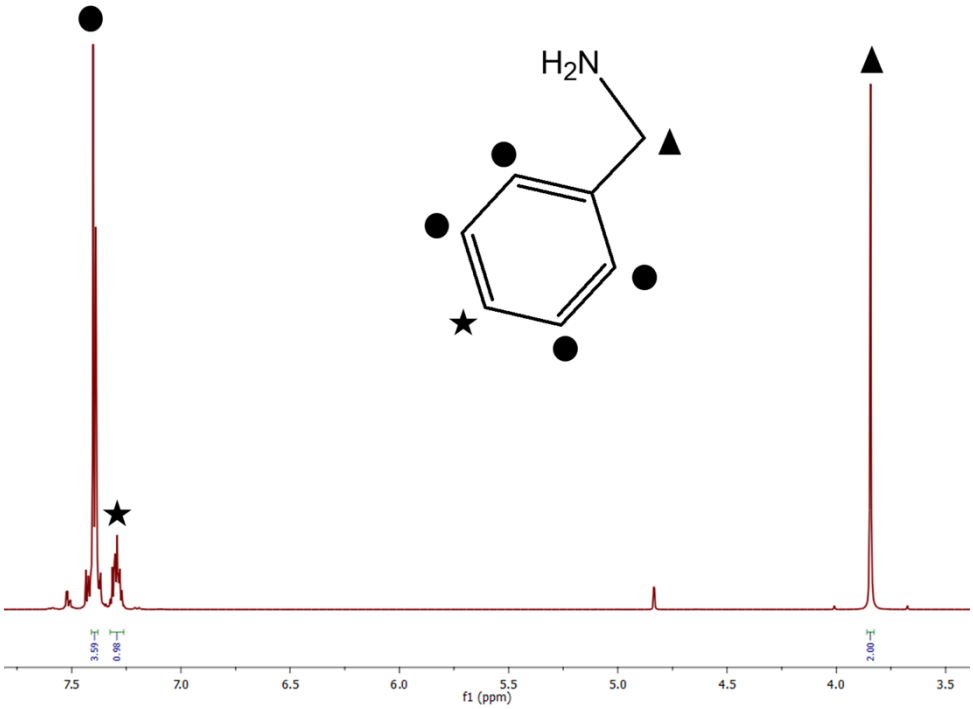

Figure S50. ^{1}H-NMR (in 400MHz) chemical shift of **benzyl amine** monomer (*N*pm) in CD_3CN.

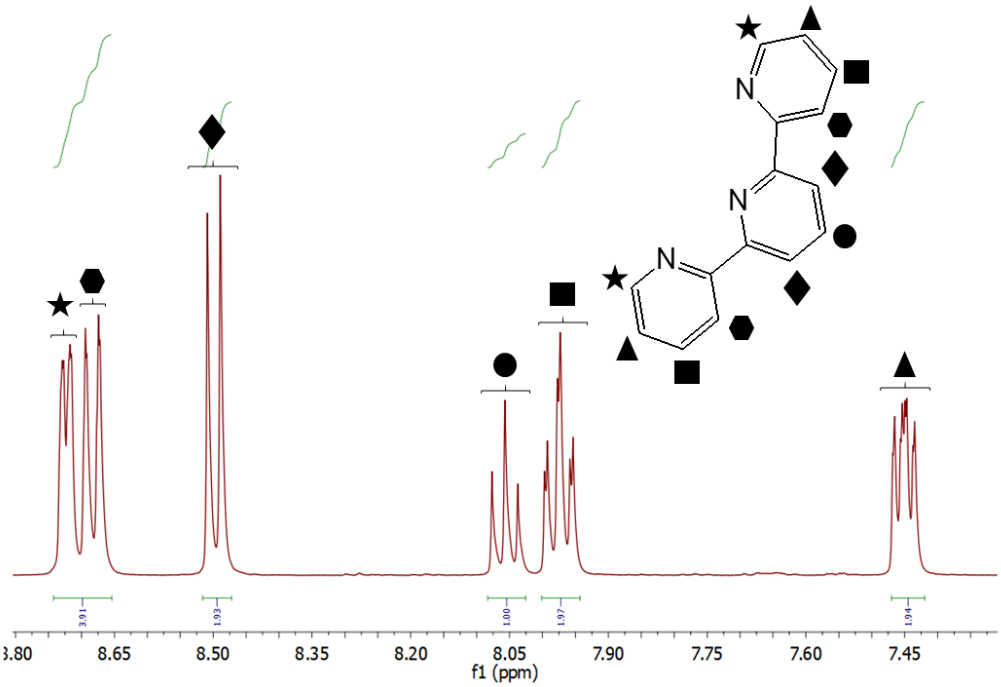

Figure S51. ^{1}H-NMR chemical shift of **terpy** (as a surrogate of Netp, the monomer used in synthesis) in CD_3CN.

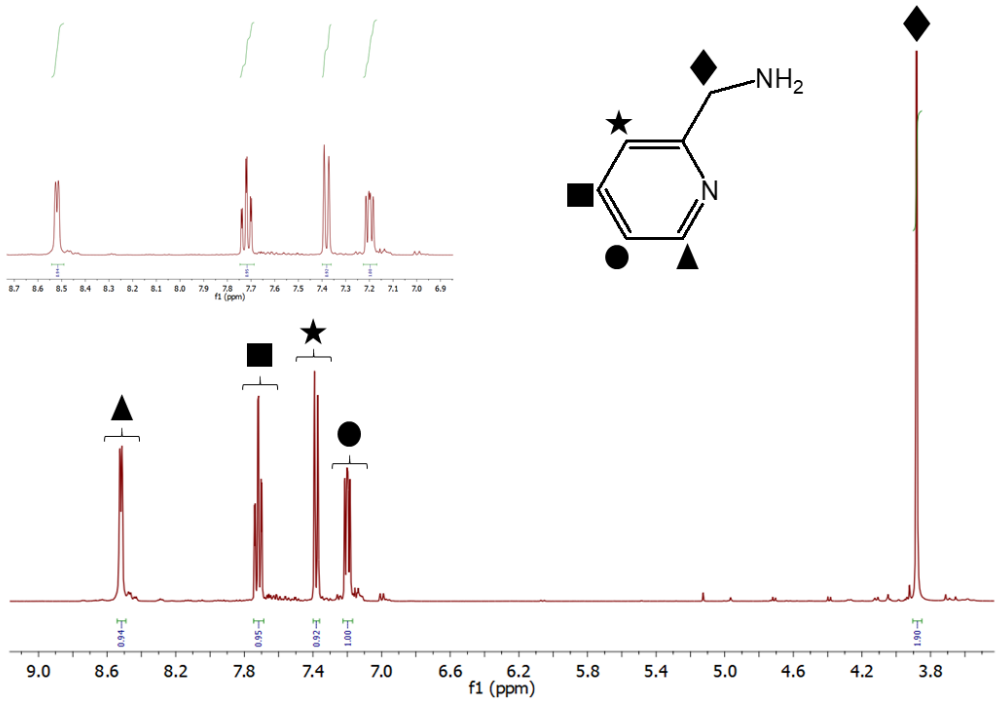

Figure S52. ^{1}H-NMR (in 400MHz) chemical shift of **2-picolyl amine** monomer (*N*pam) in CD_3CN.

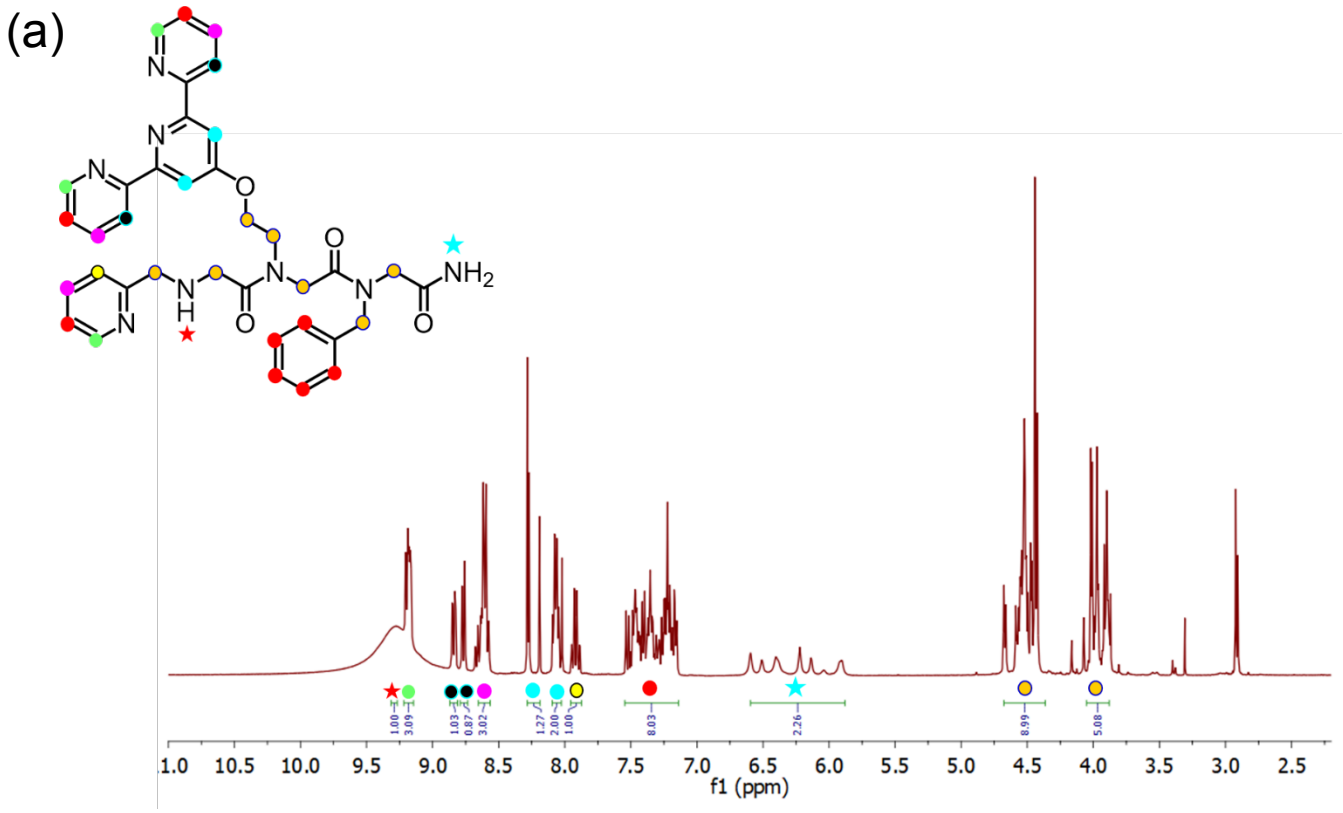

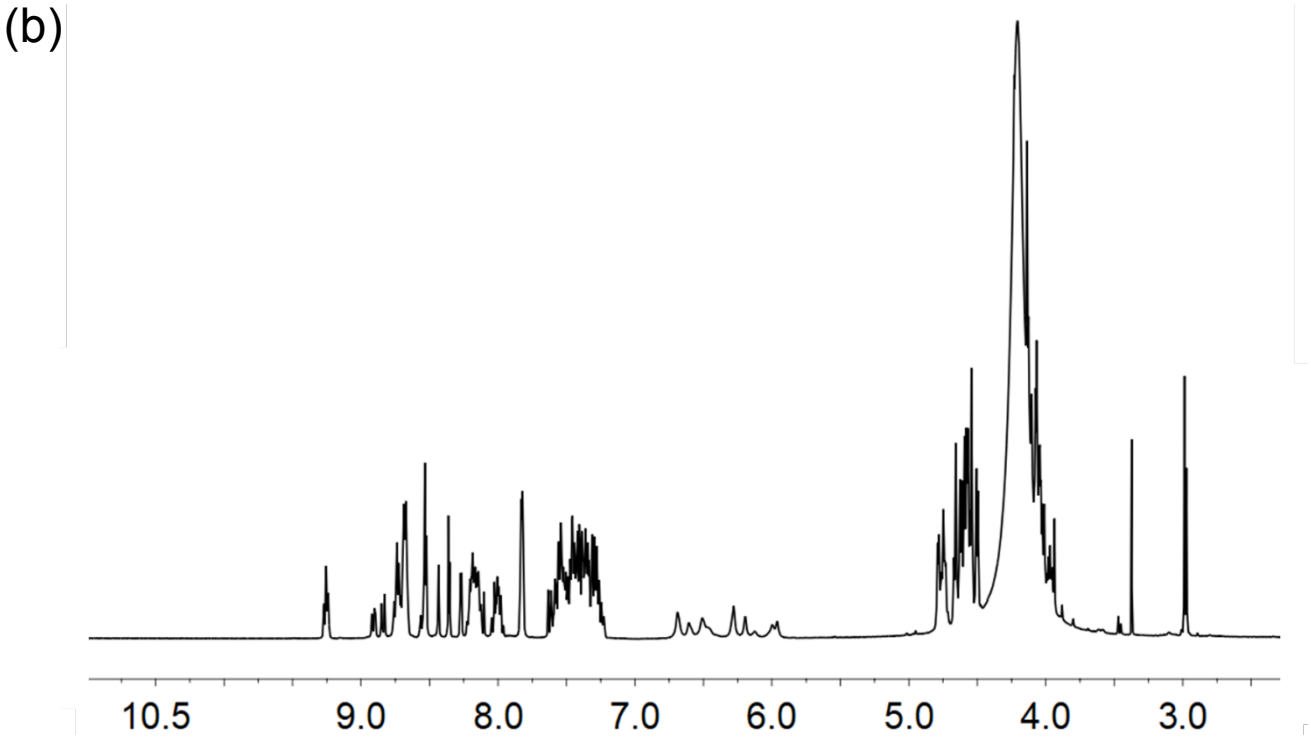

Figure S53. ^{1}H-NMR (in 400MHz) chemical shift of (a) **PT-1** ($C_{36}H_{36}N_8O_4$) and (b) Zn**PT-1** in CD_3CN. Chemical shift of *N*pm assigned near the range of 7-7.5 ppm with less acidic protons of *N*etp and *N*pam group (see Fig. S50-52), protons adjacent to pyridine groups assigned at more downfield region near 9.30 ppm. Chemical shift of other protons expected to be similar as obtained with the monomer (see Fig. S50-52). The downfield shifting expected due to coordination with Zn^{2+} ion.[10]

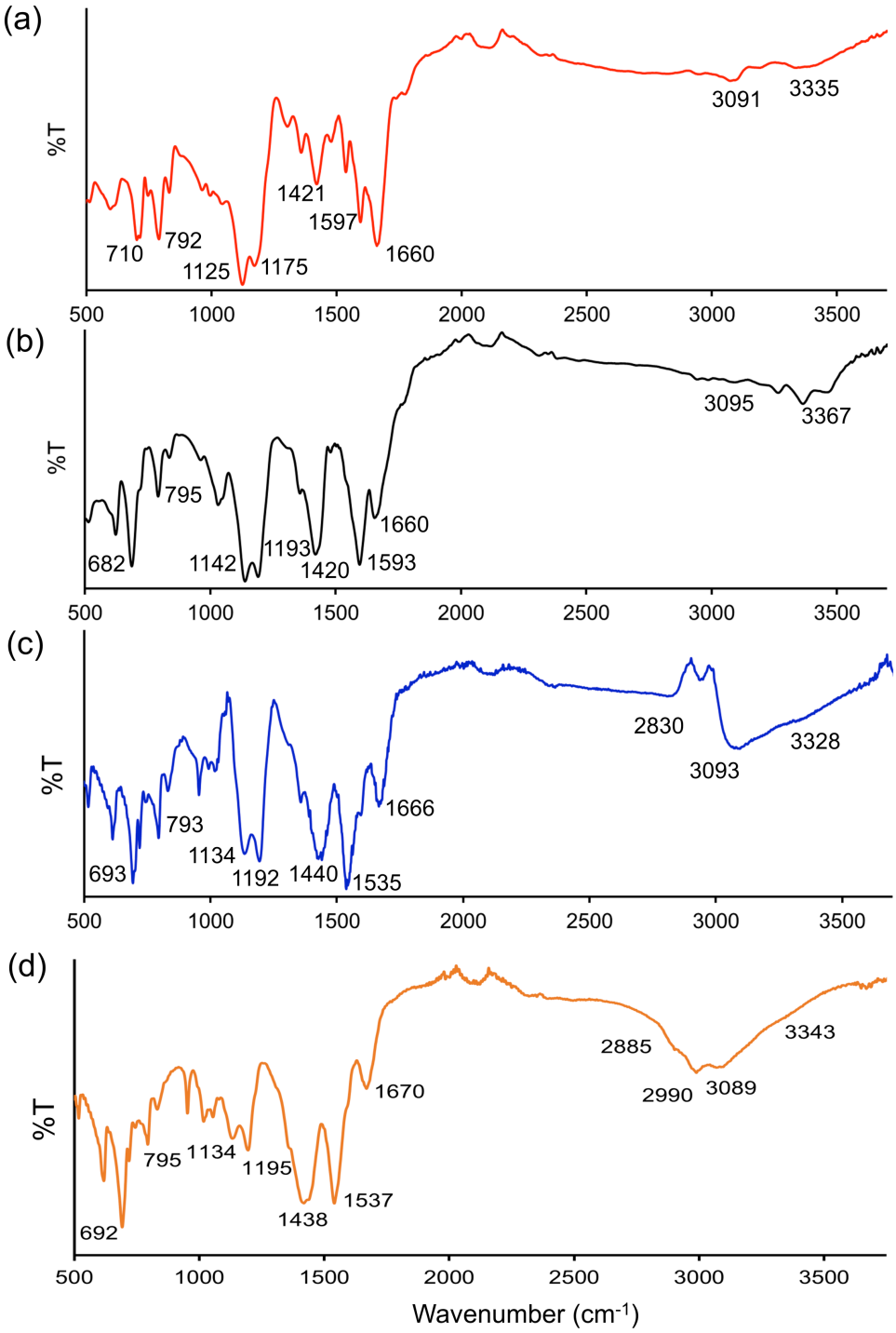
(a)
%T
710
792
1125
1175
1421
1597
1660
3091
3335
(b)
%T
682
795
1142
1193
1420
1593
1660
3095
3367
(c)
%T
693
793
1134
1192
1440
1535
1666
2830
3093
3328
(d)
%T
692
795
1134
1195
1438
1537
1670
2885
2990
3089
3343
500
1000
1500
2000
2500
3000
3500
Wavenumber (cm-1)

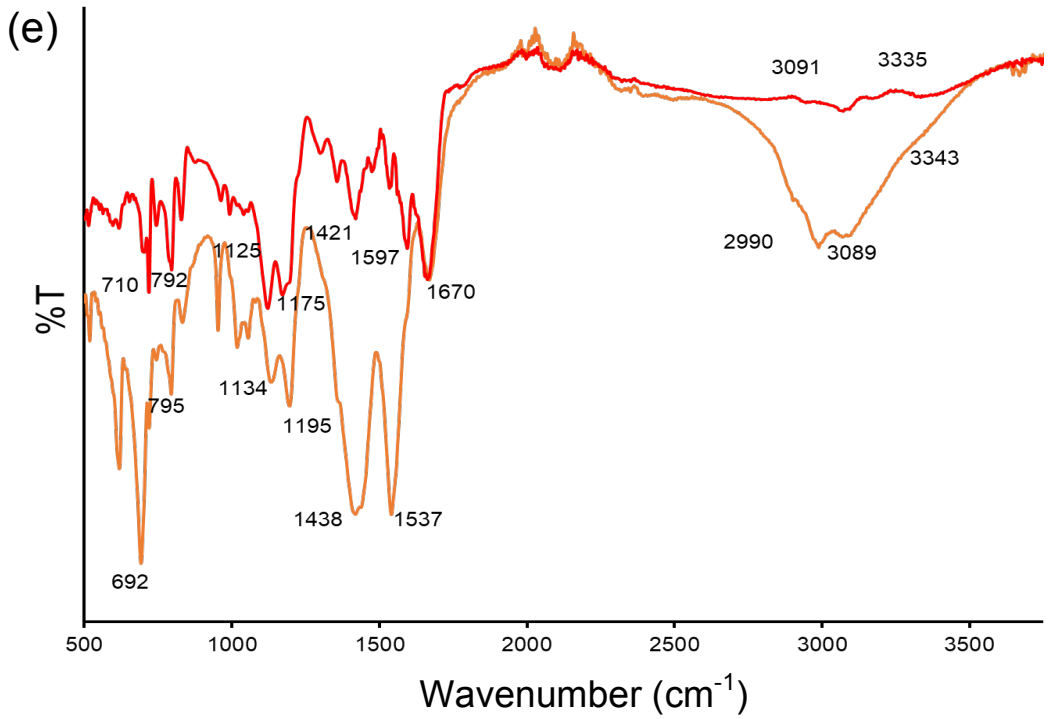

Figure S54. Solid phase FT-IR of (a) **PT-1** (red), (b) Cu**PT-1**(black)**,** (c) Zn**PT-1** (blue line, obtained from the complex synthesis in water medium) and (d) Zn**PT-1** (orange line, obtained after evaporating the CD_3CN in NMR analysis), (e) overlayed spectra of **PT-1** and Zn**PT-1** (as obtained after CD_3CN evaporation).

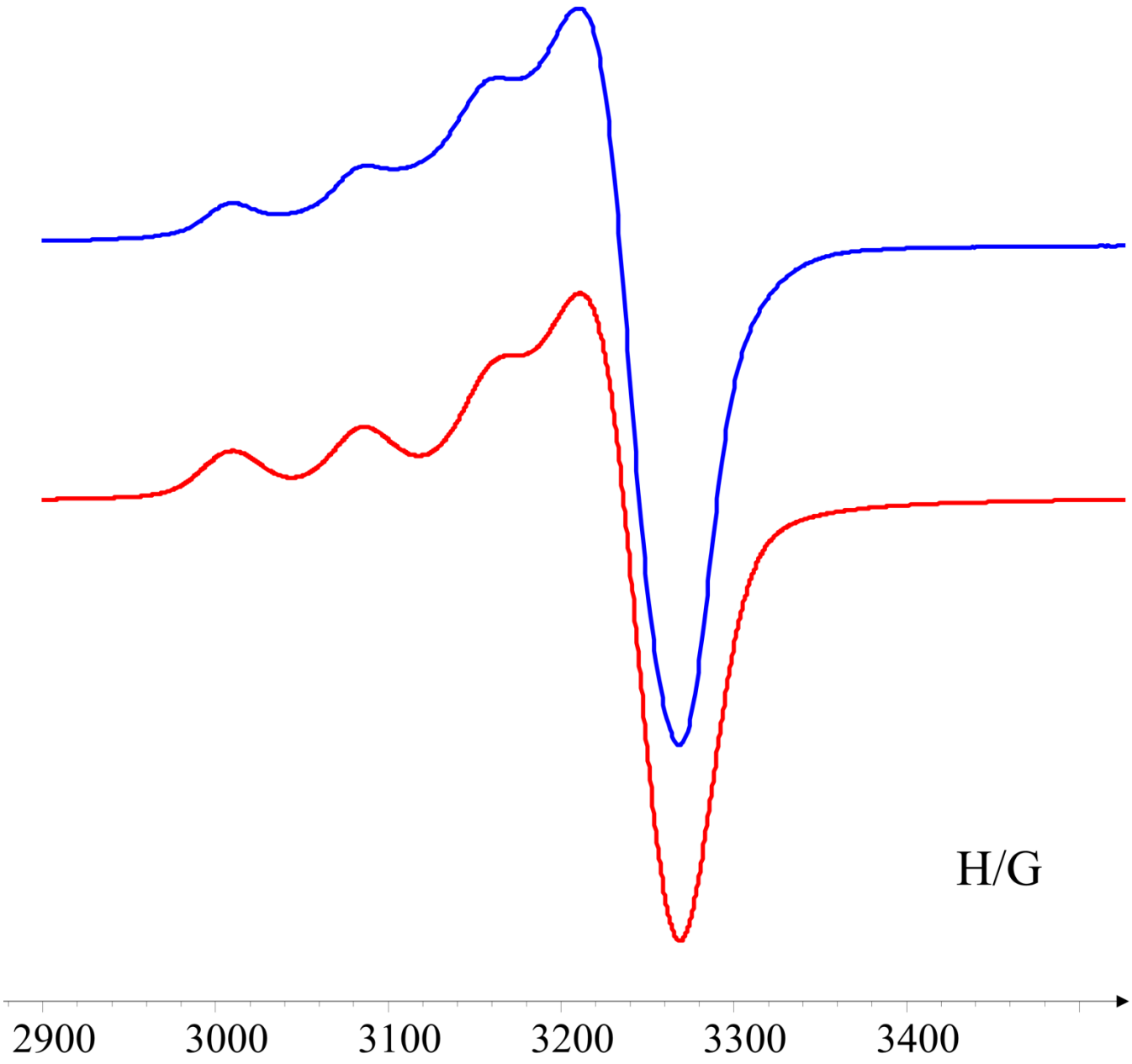

Figure S55. X-band EPR spectra of Cu**PT-1** in water (frozen solution), red: simulated and blue: experimental spectrum. Hamiltonian parameter g_{II}: 2.22; $g_{\perp}$: 2.06; A_{II}: 165G.

Peptoid is electron-donating scaffold[11] that would help in increasing the HOMO-LUMO gap.[12] Zn^{2+} and Cu^{2+} have different electronic configuration, *i.e.;* d^{10} and d^{9} respectively. The *d* orbital available for interaction with ligand centre is fully occupied for Zn^{2+} and by one electron for Cu^{2+}. Thus interaction strength of Cu^{2+} with the ligand will be higher than Zn^{2+}.[13] Electron density in HOMO-LUMO orbital shows contribution of the picolyl moiety and peptoid backbone in HOMO and terpyridine in LUMO. Complexation makes lowering the HOMO-LUMO energy (Fig. S56). The LUMO of Cu**PT-1** is more stabilized than the LUMO of Zn**PT-1**. Indeed, due to higher interaction energy equatorial ligation of Cu^{2+} with nitrogen of terpyridine and oxygen of acetate ion is stronger that results in shortening the bond distance for Cu-terpyridine than Zn terpyridine in Zn**PT-1**. The bond distances are as follows: For Cu**PT-1**, Cu49-N46, Cu49-N47, Cu49-N48 and Cu49-O52 are 2.073, 1.958, 2.088 and 1.947Å (see Fig. 6b for atom numbering). For Zn**PT-1**, Zn49-N46, Zn49-N47, Zn49-N48 and Zn49-O52 are 2.181, 2.080, 2.213 and 2.038 Å (Fig. 6a for atom numbering). The strong interaction stabilized the LUMO of Cu**PT-1**.

In case of HOMO, Cu^{2+} offers d_z^2 orbital (Fig. S56c),[14] which interacts with picolyl nitrogen and eventually raise the energy.[15] Because of the axial interaction, the bond distance is higher in Cu**PT-1**, *i.e.;* 2.371Å (Cu49-N22) than Zn**PT-1**, *i.e.;* 2.176Å (Zn49-N22). Strong interaction makes a better stabilization of Zn**PT-1** HOMO, whereas weak interaction leads to a possible destabilization of Cu**PT-1** HOMO.[16] Lowering the LUMO energy and increasing the HOMO energy for Cu**PT-1** decreases the HOMO-LUMO gap in comparison with Zn**PT-1** and thus makes the Zn**PT-1** more stable than Cu**PT-1**. Rational designing of the peptoid scaffold with proper structure directing group might help the peptoid to offer the metal ion to place the picolyl group in axial position, which in turn resulted in a discrimination in interaction eventually the stability.

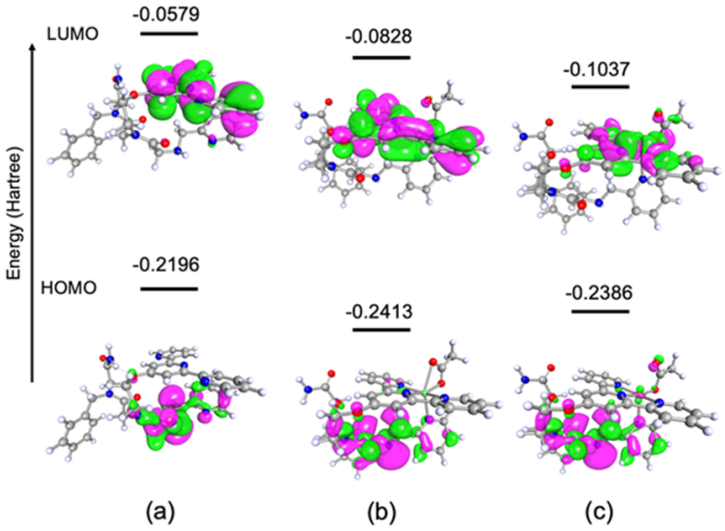

Figure S56. Image of HOMO-LUMO for (a) **PT-1**, (b) Zn**PT-1** and (c) Cu**PT-1** (iso-surface cut off: 0.02, color code: grey: carbon, blue: nitrogen, red: oxygen, white: hydrogen, green: Zn and pink: Cu).

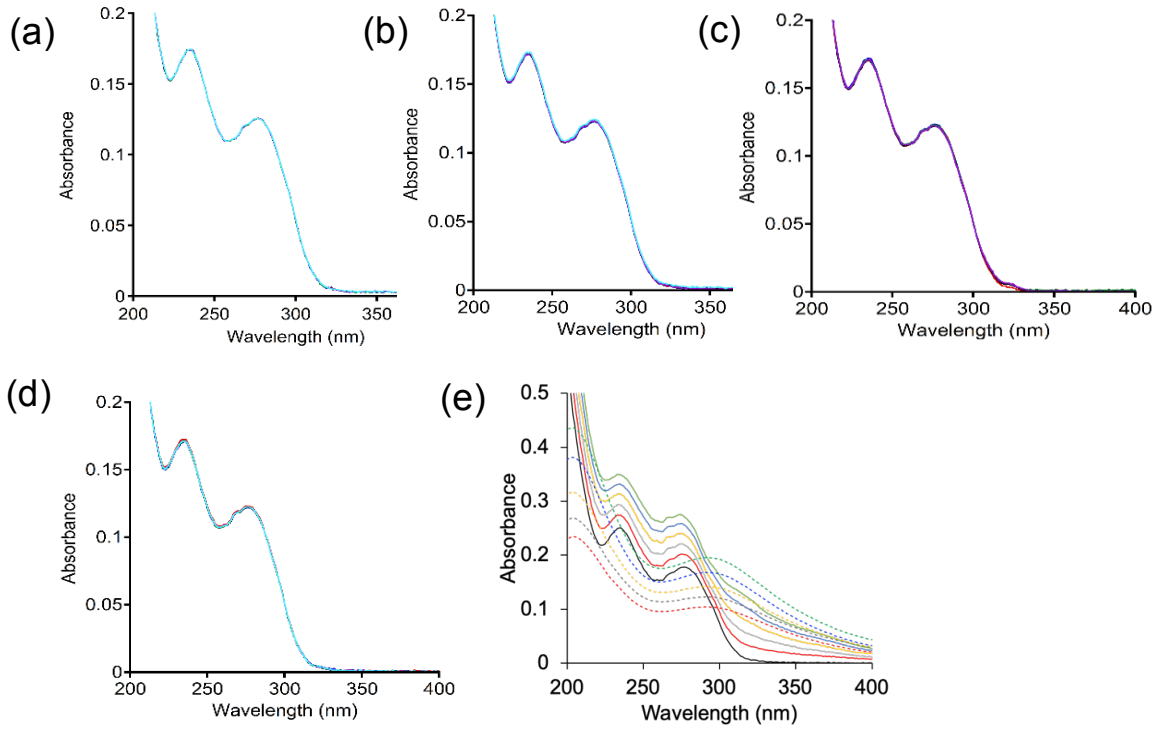

Figure S57. UV-Vis of the **PT-1** with (a) Ca^{2+}, (b) K^{+}, (c) Mg^{2+}, (d) Na^{+}, (e) Fe^{3+}, in water, 8 µM, titration was carried out by gradually adding metal ions 2µL each time. Stock solution of **PT-1** and metal ions are 5mM in water. In fig. e., the overlaid absorbance spectra of $Fe(ClO_4)_3.2H_2O$ with chelator **PT-1** (solid line) and without **PT-1** (dashed green line), indicating that the observed rise in the absorption titration spectra in presence of ligands is due to the absorption of the iron salt and not due to binding of the chelator to Fe^{3+}, as reported in literature.[17]

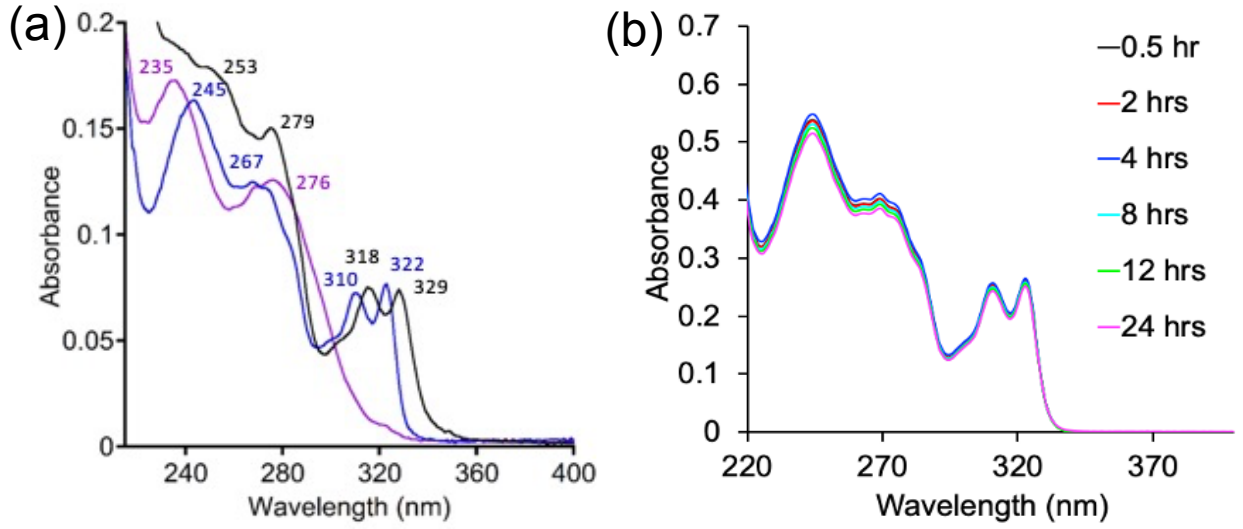

Figure S58. (a) UV-Vis of the **PT-1** (purple), Zn**PT-1** (blue) and Cu**PT-1** (black) in SBF (simulated body fluid) (6 µM), reveals that chelator **PT-1** is working perfectly in SBF, a biological like medium; (b) Zn**PT-1** complex solubilized in SBF at 37°C and monitored for 24 hours (17 µM).

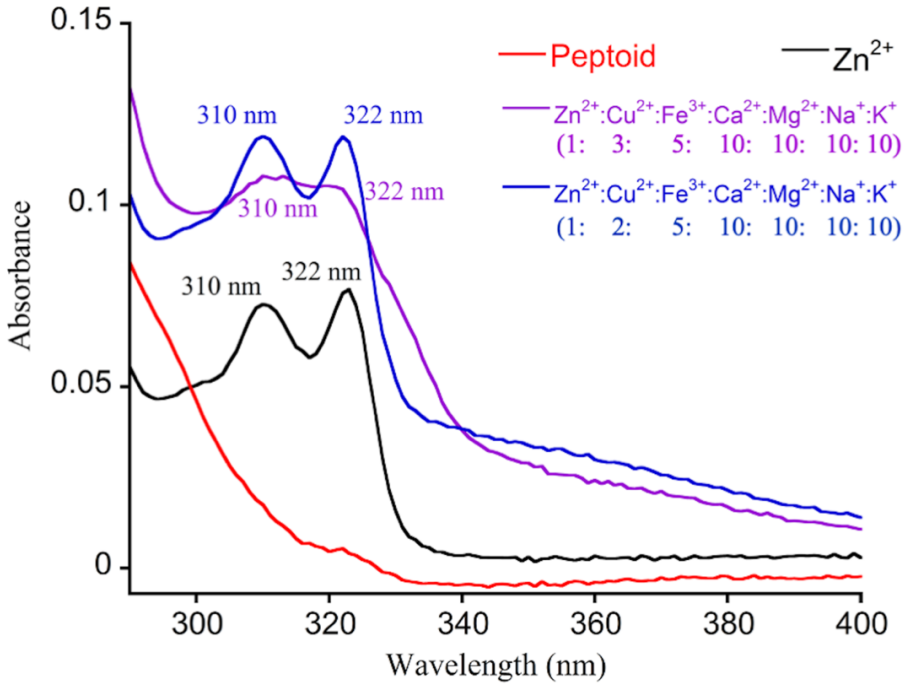

Figure S59. UV-Vis of the **PT-1** (red), Zn**PT-1** (black) and competition in varying ratio of metal ions (purple and blue, see inset) in simulated body fluid (6 µM).

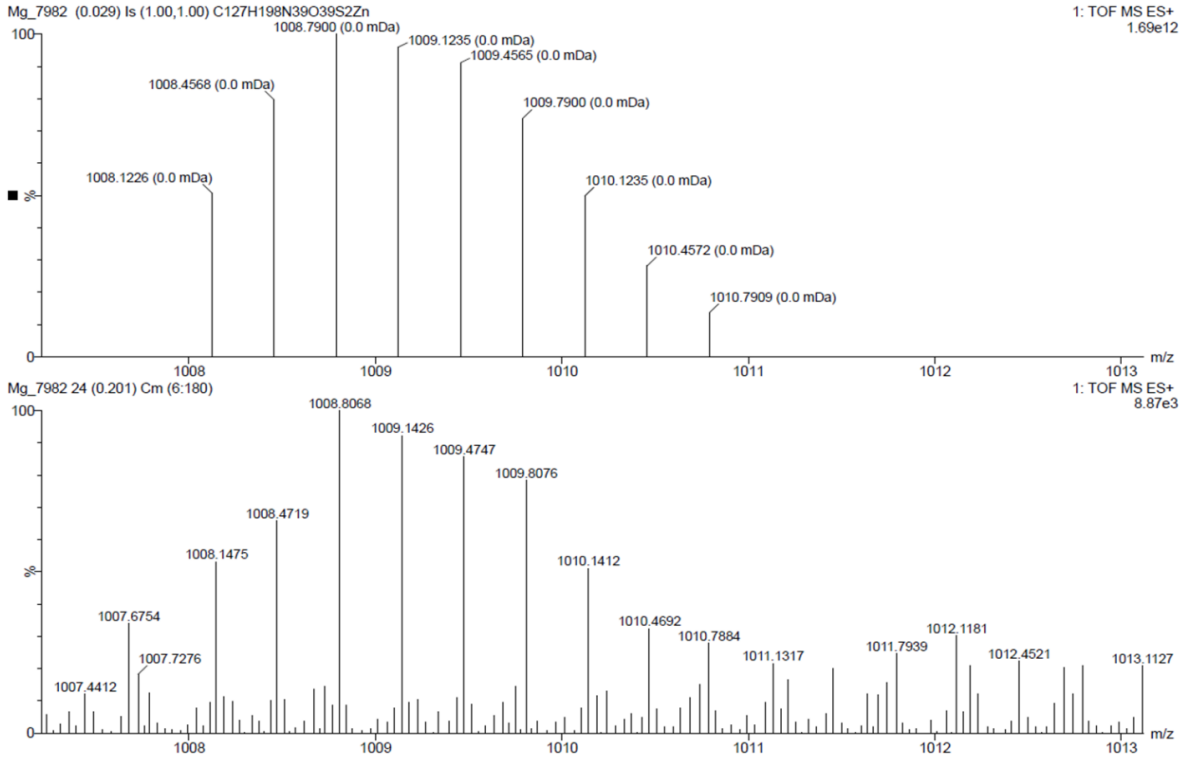

Figure S60. ESI-MS of Zinc finger protein (PYK**C**PE**C**GKSFSQKSDLVK**H**QRT**H**TG) in 3+ charge. [Above: Simulated spectrum, below: experimental spectrum].

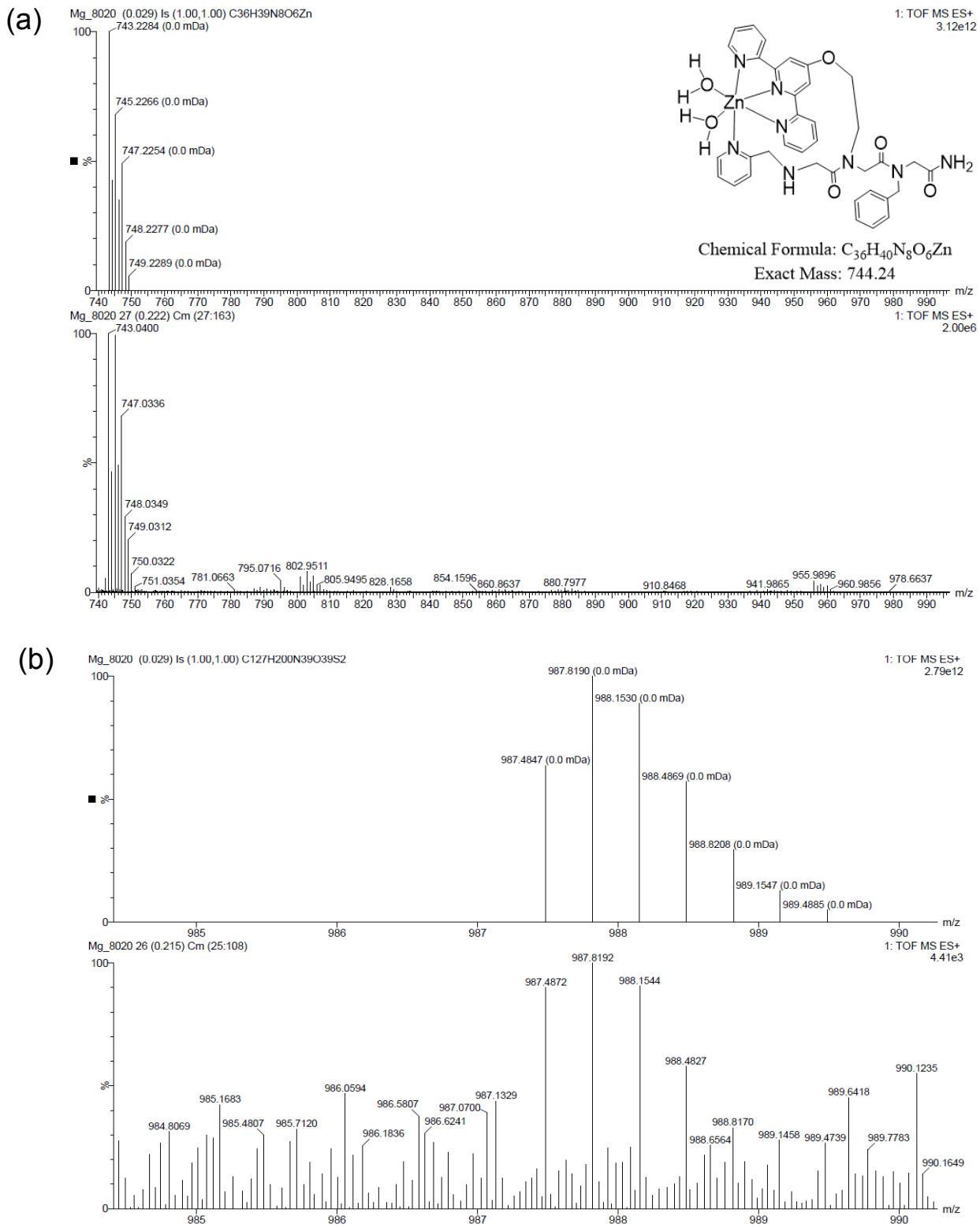

Figure S61. (a) ESI-MS of **PT-1** added Zn-ZF solution; it shows the formation of Zn**PT-1** complex (b) expanded view of the same ESI-MS file shows the presence of Apo-ZF in 3+ charge. [Top: Simulated spectrum, bottom: experimental spectrum].

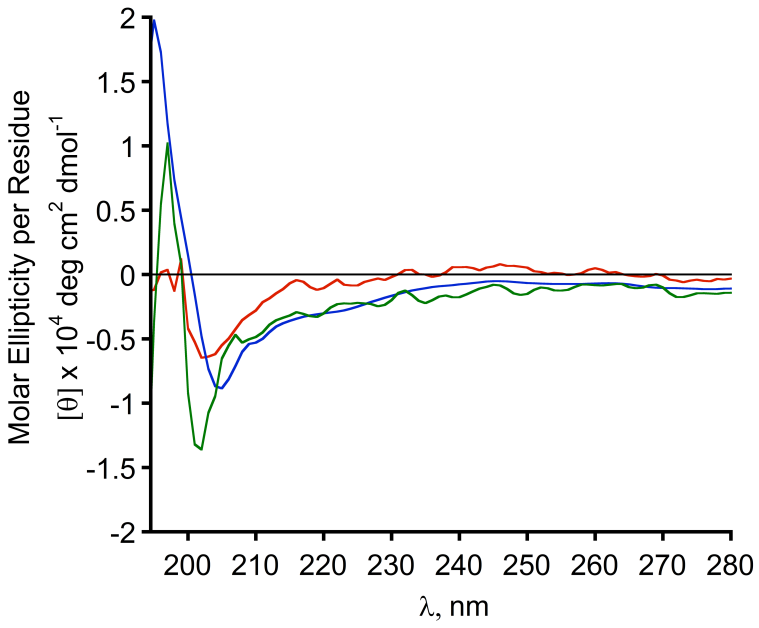

Figure S62. CD spectra of Apo-ZF (red line), Zn-ZF (blue line) and Zn^{2+} chelated ZF (green line) in acetate buffer (pH 6.5).

Table S4. Coordinates of **PT-1**.

total energy: -2129.91304869579 Hartree

C	9.0373210	6.8370819	2.5545684
C	10.3187623	6.6881271	3.0837788
C	10.9599853	7.8274421	3.5793465
C	10.3035310	9.0526687	3.5164519
C	9.0184681	9.1044549	2.9533527
C	8.2703886	10.4192118	2.9045022
C	6.1944419	11.5223508	2.3144937
C	5.6108753	11.8001891	3.7100857
C	6.1679948	14.2127279	3.4728946
C	7.6960869	14.3536776	3.3730844
C	7.7385211	15.5119377	5.5775021
C	9.7719367	15.3342673	4.1306527
C	10.6320002	14.2113819	4.7232611

C	4.8494358	13.3500395	5.4268025
C	5.2423114	12.6500761	6.7276394
N	8.4007874	8.0134273	2.4875527
N	6.9880437	10.3146508	2.2347218
N	5.6718257	13.0627902	4.2404423
N	8.3472412	15.0650218	4.3266817
N	10.6899806	13.0924974	3.9730079
O	5.0540195	10.8870360	4.3195729
O	6.6296152	12.8122837	7.0300457
O	8.3000116	13.8768855	2.4060593
O	11.1837080	14.3432633	5.8135220
N	12.0313908	11.1216986	5.8093411
N	9.4800951	9.8395714	6.4498622
N	8.6720966	7.1683690	6.2812828
C	13.3406509	11.3860504	5.8677112
C	13.9627174	11.9253478	6.9964285
C	13.1732839	12.2129832	8.1118665
C	11.8049249	11.9474131	8.0542912
C	11.2727801	11.3949842	6.8826684
C	9.8118456	11.0988185	6.7660180
C	8.8751256	12.1174579	6.9674390
C	7.5132459	11.8071166	6.8332168
C	7.1647703	10.4888189	6.5257334
C	8.1805492	9.5425311	6.3286909
C	7.8152688	8.1456300	5.9454217
C	6.6172724	7.8846611	5.2555060
C	6.3024818	6.5676065	4.9245240
C	7.1899046	5.5524251	5.2832703
C	8.3628855	5.9121003	5.9548365

H	8.4927654	5.9642315	2.1761688
H	10.7911724	5.7041211	3.1213932
H	11.9550415	7.7596193	4.0266875
H	10.7693506	9.9425211	3.9413953
H	8.8895625	11.1627714	2.3733587
H	8.1936335	10.8002017	3.9466173
H	6.7950712	12.3560571	1.9383716
H	5.3105367	11.4242279	1.6585283
H	5.7401006	15.1177076	3.9159642
H	5.8070490	14.1755107	2.4369141
H	8.5653511	15.6859149	6.2830545
H	7.1609018	14.6947066	6.0238118
H	10.0288011	16.2674333	4.6449961
H	9.9636059	15.4429185	3.0550491
H	3.8000559	13.0739281	5.2251195
H	4.8725982	14.4359677	5.5792024
H	4.6865929	13.1276240	7.5481956
H	4.9621473	11.5945376	6.6966627
H	6.4772541	9.5078675	2.5904238
H	11.1447383	12.2613838	4.3596597
H	10.1273419	13.0344596	3.1280749
H	13.9238242	11.1662593	4.9665030
H	15.0374233	12.1190010	6.9934958
H	13.6172594	12.6389832	9.0151001
H	11.1537367	12.1581205	8.9047707
H	9.1960337	13.1339371	7.1947728
H	6.1293670	10.1892900	6.4145007
H	5.9633499	8.7032223	4.9500136
H	5.3831778	6.3411336	4.3788711

H	6.9899070	4.5062806	5.0418038
H	9.0865968	5.1395427	6.2413261
C	6.8937872	16.7659053	5.4714765
C	7.0211956	17.6619839	4.4021866
C	6.2367076	18.8195774	4.3499948
C	5.3159270	19.0928338	5.3663228
C	5.1813600	18.2001840	6.4361788
C	5.9645912	17.0440133	6.4861940
H	7.7298022	17.4515563	3.5977858
H	6.3455293	19.5089946	3.5088051
H	4.7009893	19.9953095	5.3232089
H	4.4594193	18.4015897	7.2317481
H	5.8537533	16.3477708	7.3228890

Table S5. Coordinates of Zn**PT-1**.

total energy: -4137.48324721934 Hartree

C	9.9453639	9.4820546	-0.1740146
C	8.9743339	9.4233217	-1.1697087
C	7.8029655	10.1609067	-0.9953109
C	7.6603730	10.9389925	0.1534014
C	8.6873834	10.9623007	1.1020644
C	8.5919234	11.8043075	2.3478005
C	7.4730997	13.6286276	3.4815576
C	6.9916511	12.9059734	4.7374368
C	7.3097279	15.0610708	5.8994945
C	8.8103786	15.3687964	5.9237270
C	8.3708244	17.5065828	4.7143416
C	7.9850360	17.0670845	3.3132569
C	8.9295098	16.5026776	2.4414947

C	8.5510389	16.0580308	1.1721683
C	7.2202678	16.1752765	0.7529972
C	6.2751377	16.7482681	1.6092551
C	6.6576697	17.1907081	2.8804458
C	10.6918633	16.7193307	5.3325128
C	11.4358741	16.6763074	6.6680735
C	6.6104095	12.9878043	7.1452142
C	7.6996143	12.2391054	7.9118013
N	9.8070999	10.2250729	0.9384671
N	7.5180179	12.7804723	2.3106583
N	7.0188668	13.6363703	5.8974320
N	9.2436890	16.5552119	5.4149582
N	10.7956742	17.2188014	7.7184944
O	6.6411558	11.7316604	4.7182769
O	7.9233610	10.9153785	7.3970829
O	9.6043772	14.5690283	6.4149919
O	12.5774694	16.2237338	6.7189255
C	13.0227045	12.3752000	2.4714502
C	13.5566816	13.5441443	3.0193118
C	13.0840975	13.9711133	4.2613121
C	12.1011486	13.2218945	4.9123975
C	11.6200351	12.0625472	4.2988816
C	10.5817370	11.1854047	4.9069223
C	9.7769936	11.5667722	5.9770951
C	8.7968073	10.6634027	6.4213721
C	8.7007928	9.3967642	5.8128628
C	9.5329412	9.1092921	4.7379994
C	9.4930586	7.8442782	3.9531249
C	8.7358673	6.7305146	4.3288932

C	8.7843491	5.5847561	3.5326905
C	9.5859421	5.5800792	2.3896020
C	10.3071964	6.7351425	2.0826466
N	12.0822574	11.6628470	3.0958752
N	10.4358371	10.0011465	4.3063483
N	10.2539841	7.8302786	2.8420925
Zn	11.3068388	9.7340334	2.4360711
C	14.8422000	8.0622823	1.3877848
C	13.5676337	8.6588825	1.9393014
O	12.7127049	9.1185296	1.0952130
O	13.3463456	8.7126212	3.1662650
H	15.4012080	8.8381584	0.8405859
H	9.1392707	8.8079326	-2.0554704
H	7.0086831	10.1338449	-1.7450587
H	6.7602982	11.5266239	0.3321142
H	9.5839790	12.2692356	2.5150598
H	8.4060992	11.1383801	3.2025988
H	8.4581454	14.0847416	3.7141393
H	6.7933414	14.4675534	3.2732020
H	6.8713813	15.5085627	6.8044694
H	6.8137142	15.5481926	5.0534582
H	8.9099141	18.4646369	4.6799431
H	7.4687447	17.6931436	5.3129080
H	9.9703920	16.3957376	2.7519732
H	9.2987353	15.6192332	0.5064812
H	6.9227205	15.8232009	-0.2378313
H	5.2336432	16.8431118	1.2925871
H	5.9094176	17.6226849	3.5508981
H	10.9035151	17.6900968	4.8632938

H	11.1416484	15.9364525	4.7066453
H	5.7924009	12.2863226	6.9266290
H	6.2173319	13.7675106	7.8127967
H	8.6311633	12.8190797	7.9526618
H	7.3460885	12.0744599	8.9386777
H	7.6224134	13.3843708	1.4958042
H	11.2341876	17.2111383	8.6339046
H	9.8401306	17.5475307	7.6457208
H	13.3573180	11.9951801	1.5022275
H	14.3240775	14.0999676	2.4782768
H	13.4598924	14.8788661	4.7385445
H	11.7170573	13.5488768	5.8764883
H	9.8530941	12.5687111	6.3893129
H	7.9387217	8.7020885	6.1626366
H	8.1252263	6.7491902	5.2315115
H	8.2033424	4.7019466	3.8079637
H	9.6554904	4.7027130	1.7447240
H	10.9517864	6.7856636	1.2008788
H	10.8779850	8.9210026	-0.2600840
H	14.5965060	7.2693560	0.6643931
H	15.4693981	7.6553204	2.1910972

Table S6. Coordinates of Cu**PT-1**.

total energy: -3998.58066618600 Hartree

C	9.8794519	9.4102548	-0.0014379
C	8.8748201	9.2638560	-0.9576067
C	7.6834972	9.9676254	-0.7763643
C	7.5548285	10.7982750	0.3373594
C	8.6192797	10.9005816	1.2408063

C	8.5459190	11.7953912	2.4514853
C	7.4245300	13.6372700	3.5503049
C	6.9791416	12.9394371	4.8337292
C	7.3498958	15.1102009	5.9476252
C	8.8506553	15.4124697	5.8912187
C	8.3518516	17.5367316	4.6814906
C	7.8864149	17.0819374	3.3098874
C	8.7808388	16.5120122	2.3903006
C	8.3307240	16.0514811	1.1504049
C	6.9771037	16.1583722	0.8088958
C	6.0811051	16.7374861	1.7124887
C	6.5352765	17.1956544	2.9541939
C	10.7014661	16.7484094	5.1797229
C	11.5162754	16.7289362	6.4737203
C	6.6871074	13.0584762	7.2508729
C	7.7954287	12.2957863	7.9732998
N	9.7569727	10.1998188	1.0752064
N	7.4596911	12.7572365	2.4044541
N	7.0550533	13.6869513	5.9808737
N	9.2597674	16.5897841	5.3434438
N	10.9341147	17.2921768	7.5465404
O	6.6154784	11.7692744	4.8469023
O	7.9872693	10.9730917	7.4406208
O	9.6665646	14.6161560	6.3523026
O	12.6579305	16.2733709	6.4716611
C	13.1865727	12.1384812	2.5193495
C	13.6850877	13.3680871	2.9580461
C	13.1502809	13.9304041	4.1179124
C	12.1350920	13.2548253	4.8006173

C	11.6894354	12.0307983	4.3017243
C	10.6293382	11.2085673	4.9334880
C	9.8264675	11.6061897	5.9966080
C	8.8432056	10.7106234	6.4556935
C	8.7321189	9.4359273	5.8604312
C	9.5609292	9.1273032	4.7914040
C	9.5560344	7.8643029	4.0144509
C	8.7420109	6.7687192	4.3043911
C	8.8427814	5.6269743	3.5059890
C	9.7494600	5.6117675	2.4450702
C	10.5254507	6.7493025	2.2145194
N	12.2207220	11.4954282	3.1771243
N	10.4670822	10.0148048	4.3523398
N	10.4249737	7.8376899	2.9781077
Cu	11.4161441	9.6512642	2.6782342
C	14.7697250	8.1011237	0.9007966
C	13.6861050	8.5885060	1.8421382
O	12.6512427	9.1191328	1.2701173
O	13.7917319	8.4851746	3.0703974
H	15.1413093	8.9434658	0.2958775
H	9.0291429	8.6104936	-1.8183525
H	6.8641217	9.8746835	-1.4935121
H	6.6420412	11.3649452	0.5218711
H	9.5386816	12.2746835	2.5746317
H	8.3882454	11.1631163	3.3362708
H	8.4070581	14.1138575	3.7494409
H	6.7269327	14.4606758	3.3368680
H	6.9586972	15.5728553	6.8664068
H	6.8142253	15.5862507	5.1195583

H	8.8917035	18.4919196	4.6055446
H	7.4857506	17.7338270	5.3278376
H	9.8387444	16.4130487	2.6399808
H	9.0404311	15.6082594	0.4472070
H	6.6235903	15.7931545	-0.1585496
H	5.0224373	16.8248334	1.4563030
H	5.8255011	17.6323837	3.6624380
H	10.8888125	17.7101318	4.6823003
H	11.1162101	15.9545080	4.5429895
H	5.8465829	12.3715422	7.0754574
H	6.3403146	13.8507889	7.9290381
H	8.7338223	12.8658563	7.9832127
H	7.4788938	12.1272996	9.0115169
H	7.5378351	13.3352406	1.5684197
H	11.4217793	17.3020302	8.4367419
H	9.9772233	17.6235757	7.5187591
H	13.5660076	11.6510925	1.6178977
H	14.4774497	13.8646068	2.3959523
H	13.5028481	14.8876662	4.5086251
H	11.6966249	13.6863560	5.6987586
H	9.9157242	12.6101917	6.4022890
H	7.9733911	8.7455129	6.2262149
H	8.0433964	6.8018851	5.1405802
H	8.2172815	4.7565845	3.7146514
H	9.8592862	4.7376906	1.8015251
H	11.2469241	6.7949515	1.3955460
H	10.8315594	8.8824456	-0.0961981
H	14.3500912	7.3610258	0.2013514
H	15.6006045	7.6537060	1.4615580

References

[1] (a) M. Baskin and G. Maayan, A rationally designed metal-binding helical peptoid for selective recognition processes, *Chem. Sci.*, **2016**, *7*, 2809-2820.

[2] R. N. Zuckermann, J. M. Kerr, S. B. W. Kent, W. H. Moos, *J. Am. Chem. Soc.* **1992**, *114*, 10646–10647.

[3] Timothy S. Burkoth, Aaron T. Fafarman, Deborah H. Charych, Michael D. Connolly, and Ronald N. Zuckermann, *J. Am. Chem. Soc.* **2003**, *125*, 8841-8845.

[4] L. Zhang, M. Koay, M. J. Maher, Z. Xiao, A. G. Wedd, *J. Am. Chem. Soc.* **2006**, *128*, 5834–5850.

[5] A. E. Martell, R. M. Smith and R. J. Motekaitis, NIST critically selected stability constants of metal complexes, Standard reference database 46, 2001.

[6] A. Laskay, C. Garino, Y. O. Tsybin, L. Salassa, A. Casini, *Chem. Commun.* **2015**, *51*, 1612–1615.

[7] M. A. Franzman, A. M. Barrios, *Inorg. Chem.* **2008**, *47*, 3928–3930.

[8] P. Ghosh, N. Fridman and G. Maayan, **2020**, submitted elsewhere.

[9] K. F. Bowes, I. P. Clark, J. M. Cole, M. Gourlay, A. M. E. Griffin, M. F. Mahon, L. Ooi, A. W. Parker, P. R. Raithby, H. A. Sparkes, et al., *CrystEngComm* **2005**, *7*, 269–275.

[10] Q-X. Geng, H. Cong, Z. Tao, L. F. Lindoy, G. Wei, *Supramol. Chem.*, **2016**, *28*, 784-791.

[11] Baskin, M.; Panz, L.; Maayan, G. Versatile Ruthenium Complexes Based on 2,2′-Bipyridine Modified Peptoids. *Chemical Communications* **2016**, *52* (68), 10350–10353. https://doi.org/10.1039/c6cc04346a.

[12] Rillema, D. P.; Stoyanov, S. R.; Cruz, A. J.; Nguyen, H.; Moore, C.; Huang, W.; Siam, K.; Jehan, A.; Komreddy, V. HOMO-LUMO Energy Gap Control in Platinum(II) Biphenyl Complexes Containing 2,2′-Bipyridine Ligands. *Dalton Transactions* **2015**, *44* (39), 17075–17090. https://doi.org/10.1039/c5dt01891a.

[13] Matsubara, T.; Hirao, K. Density functional study of the binding of the cyclen-coordinated M(II) (M=Zn, Cu, Ni) complexes to the DNA base. Why is Zn better to bind? *J. Mol. Struct. (TheoChem)*, **2002**, *581*, 203-213.

[14] Freitag, R.; Conradie, J. Understanding the Jahn-Teller Effect in Octahedral Transition-Metal Complexes: A Molecular Orbital View of the Mn(β-Diketonato)3 Complex. *Journal of Chemical Education* **2013**, *90* (12), 1692–1696. https://doi.org/10.1021/ed400370p.

[15] Cheng, R-J.; Chen, P-Y.; Lovell, T.; Liu, T.; Noodleman, L.; Case, D. A. Symmetry and Bonding in Metalloporphyrins. A Modern Implementation for the Bonding Analyses of Five- and Six-Coordinate High-Spin Iron(III)-Porphyrin Complexes
through Density Functional Calculation and NMR Spectroscopy, *J. Am. Chem. Soc.* **2003**, *125*, 6774-6783. https://doi.org/ 10.1021/ja021344n.

[16] Solomon, E. I.; Szilagyi, R. K.; DeBeer George, S.; Basumallick, L. Electronic Structures of Metal Sites in Proteins and Models: Contributions to Function in Blue Copper Proteins. *Chemical Reviews* **2004**, *104* (2), 419–458. https://doi.org/10.1021/cr0206317.

[17] A. Rakshit, K. Khatua, V. Shanbhag, P. Comba and A. Datta, *Chem. Sci.*, **2018**, *9*, 7916-7930.